Visualization and Quantification of Blood Flow in the Human Aorta. From in vivo 4D Phase Contrast MRI to Subject-Specific Computational Hemodynamics

Umberto Morbiducci

Industrial Bioengineering Group
Department of Mechanics, Politecnico di Torino, Italy

Insight into the Physiological Relevance of Helical Blood Flow in the Human Aorta

Umberto Morbiducci

R Ponzini, G Rizzo, M Cadioli, A Esposito, FM Montevecchi, A Redaelli

Politecnico di Torino, Italy

CILEA, Italy

IBFM CNR, Italy

Philips Medical Systems, Italy

Institute H S. Raffaele, Italy

Politecnico di Milano, Italy

Background

Blood flow in the aorta is highly complex

In the past massive observations demonstrated

However, there is a relative paucity of in vivo quantitative data regarding helical blood flow dynamics in the human aorta.

- that helical flows predominate in areas from the ascending aorta to the aortic arch

(Segadal & Matre, 1987; Kilner et al., 1993; Chandran 1993)

- that this form of blood flow is a basic pattern for almost all the subjects no matter age and gender

(Bogren & Buonocore, 1999; Houston et al., 2003)

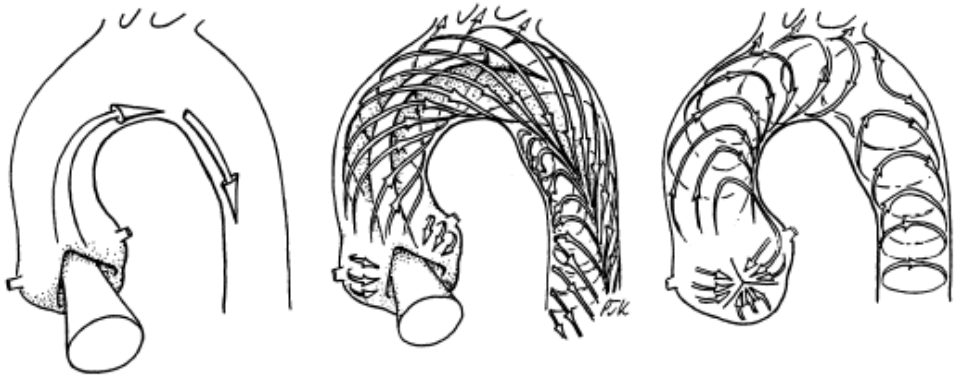

Kilner et al. *Circulation* 1993

Reference Framework

It has been proposed that energetic constraint is but one consequence of the process of physiological evolution of helical blood flow in aorta, and that others remain to be discovered.

However, there is a relative paucity of quantitative data regarding helical blood flow dynamics in the human aorta.

Qualitative Observations

NOT QUANTITATIVE

Rationale, Aim, How

Rationale

Study of mechanistic relationship between physiological complexity and energy of aortic flow

Aim

Identify common features in physiological aortic bulk flow topology

How

In vivo aortic helical flow quantification in 5 healthy humans by applying **4D PC MRI**

By using a **Lagrangian** representation of the aortic flow, we apply an index for helical flow quantification

4D PC MRI Data Acquisition

- **Five healthy volunteers (men; age 23-42 years)**
- **HR range 43-78 bpm**
- Philips Achieva 1.5 T scanner (Philips Healthcare)
- **TR=5.4 ms, TE=3ms, flip angle=15°, velocity encoding = 150 cm/s**
- **Navigator-echo** to further reduce motion artefacts

- **21 cardiac phases**
- **3C data acquired in 20-22 sagittal slices aligned with the aortic arch**
- **FOV = 280x280 mm**
- **Isotropic spatial sampling (Voxel Size 2x2x4 mm, slice spacing 2 mm)**

Theoretical Remarks on Helicity

A better understanding of the role of pitch and torsion in blood flow development can be obtained through **helicity**, a scalar eligible to study relationships between complexity and energy.

Roughly speaking, **helicity gives measure of alignment of velocity and vorticity**

Like energy, **helicity influences evolution and stability of both turbulent and laminar flows** (Moffatt and Tsinober, 1992).

Helicity related to the **reduction** of non-linear processes responsible for transfer and redistribution of energy through various scales, and hence **energy dissipation**

Helical Blood Flow: Algorithms

Particle traces computed by time integration of the velocity field (4th-order Runge-Kutta)

Sets of *Np* immaterial particles released at 5 different phase in systole and tracked up to end systole. No real tracer used.

Bicubic spline interpolation both in the spatial and time domain.

FDM implemented for velocity gradients calculation

Accuracy algorithms tested on synthetic 4D flow data mimicking a virtual PC-MRI acquisition (Morbiducci et al., 2009; Ponzini et al., 2009; Morbiducci et al., 2011).

In Vivo Quantitative Helical Blood Flow - the First Study

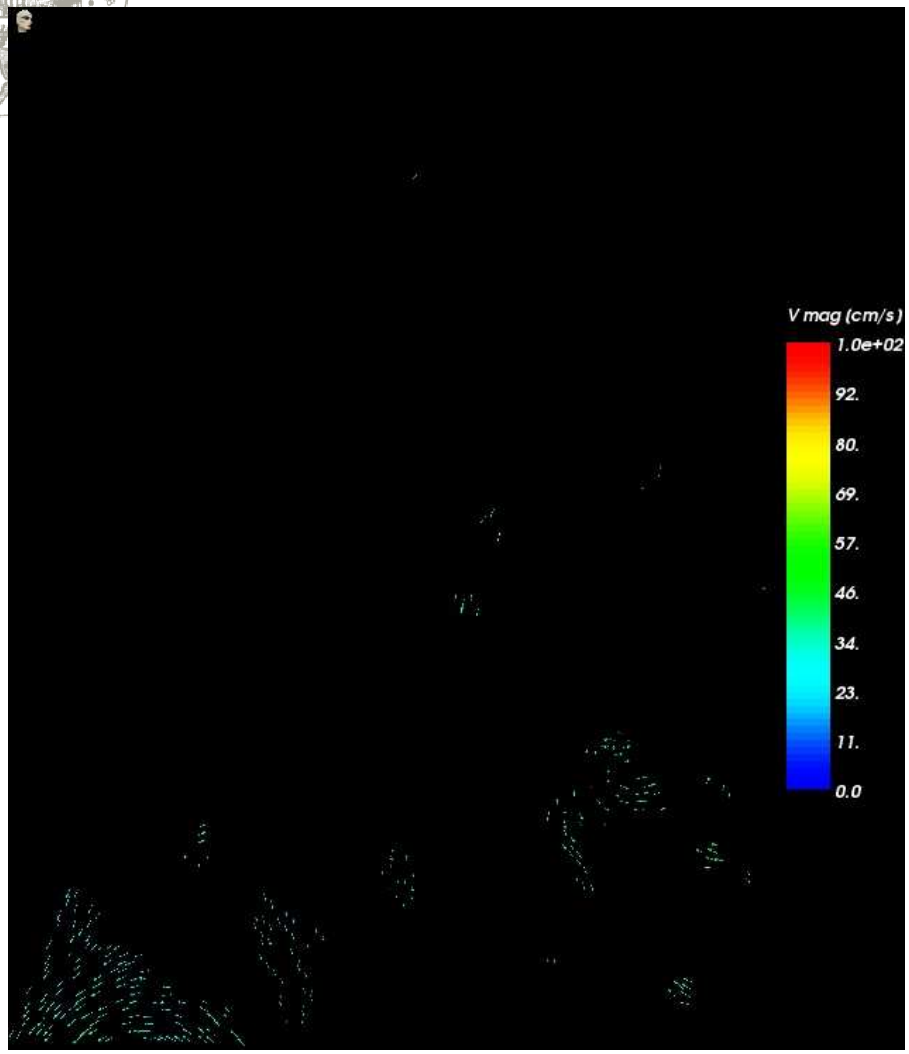

Detailed Analysis on One Healthy Subject

Morbiducci et al. *Annals of Biomedical Engineering* 2009

Helical Flow Index - HFI

Morbiducci et al. *J Biomech 2007*
Morbiducci et al. *Ann Biomed Eng 2009*
Morbiducci et al. *Ann Biomed Eng 2010*
Morbiducci et al. *Biomech Mod Mechanobiol 2011*

begins with:

LAGRANGIAN ANALYSIS

$$H_v(\mathbf{s};t) = \mathbf{V}\cdot(\nabla \times \mathbf{V}) = \mathbf{V}(\mathbf{s};t)\cdot\boldsymbol{\omega}(\mathbf{s};t)$$

$$\mathbf{LNH}(\mathbf{s};t) = \frac{\mathbf{V}(\mathbf{s};t)\cdot\boldsymbol{\omega}(\mathbf{s};t)}{\left|\mathbf{V}(\mathbf{s};t)\right|\left|\boldsymbol{\omega}(\mathbf{s};t)\right|} \qquad -1 \le \mathbf{LNH} \le 1$$

ends up with:

$$\mathrm{HFI} = \frac{1}{N_p}\sum_{k=1}^{N_p}\frac{1}{(t_k^{end} - t_k^{start})}\int_{t_k^{start}}^{t_k^{end}}\left|\mathrm{LNH}_k(\varsigma)\right|d\varsigma = \frac{1}{N_p}\sum_{k=1}^{N_p} hfi_k \qquad 0 \le \mathbf{HFI} \le 1$$

Results – Acquired PC MRI Data

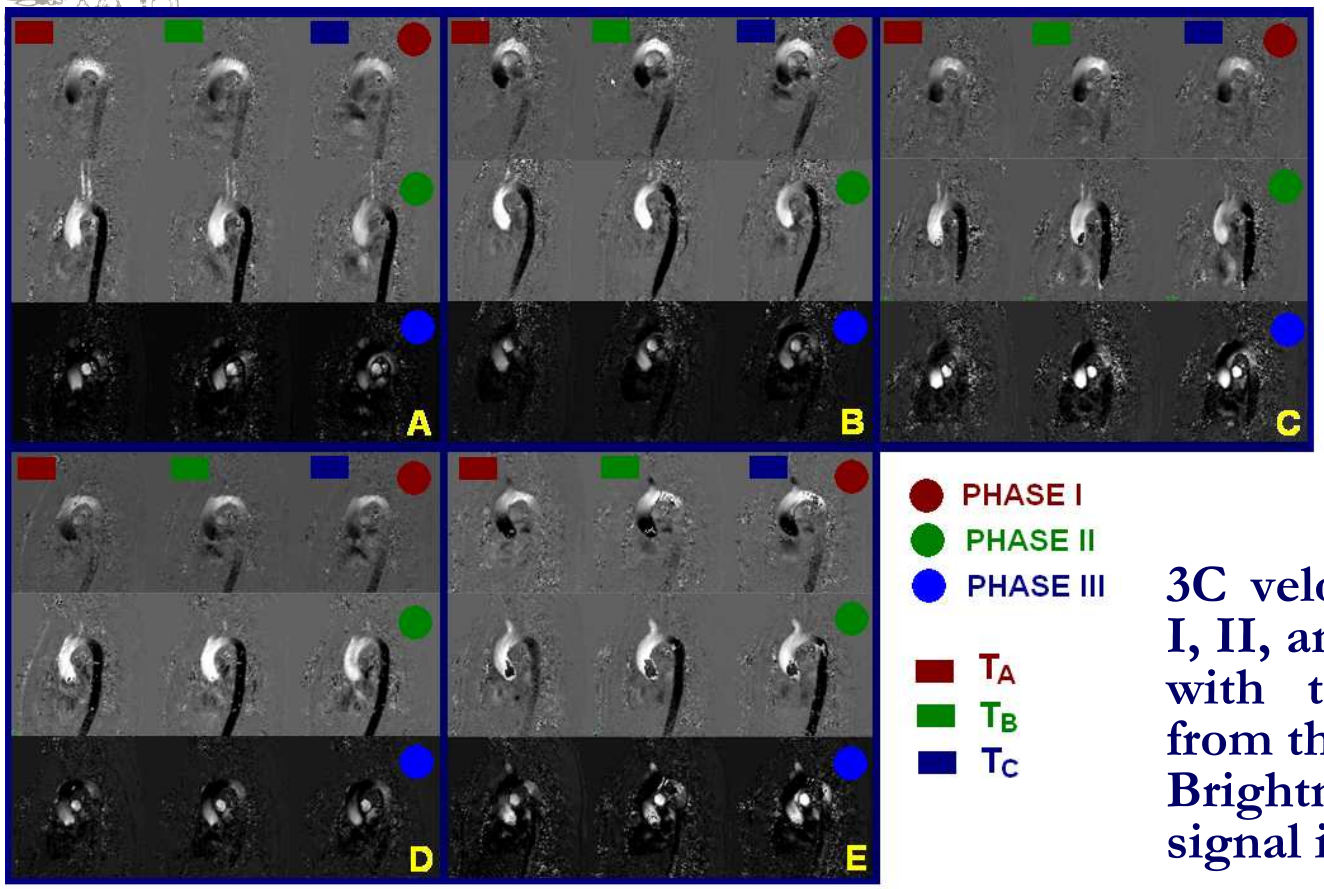

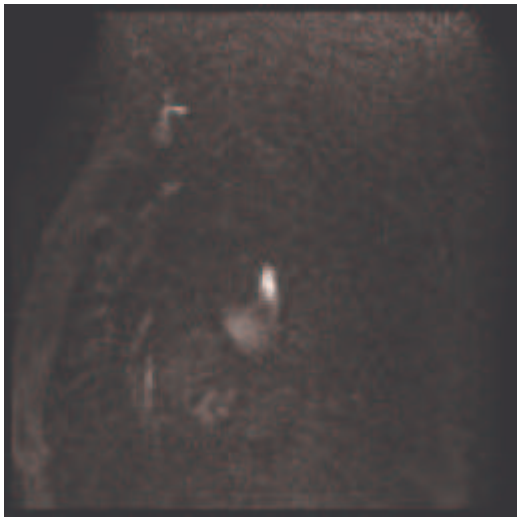

3C velocity map frames (phase I, II, and III) on a plane aligned with the aortic arch, viewed from the left.
Brightness is proportional to signal intensity

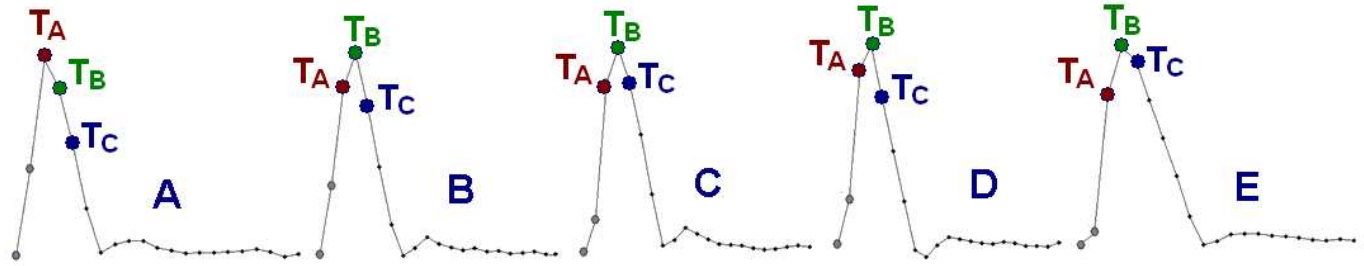

Results – Acquired PC MRI Data

Anatomical reconstruction of the aortas, together with the measured blood flow rate waveforms

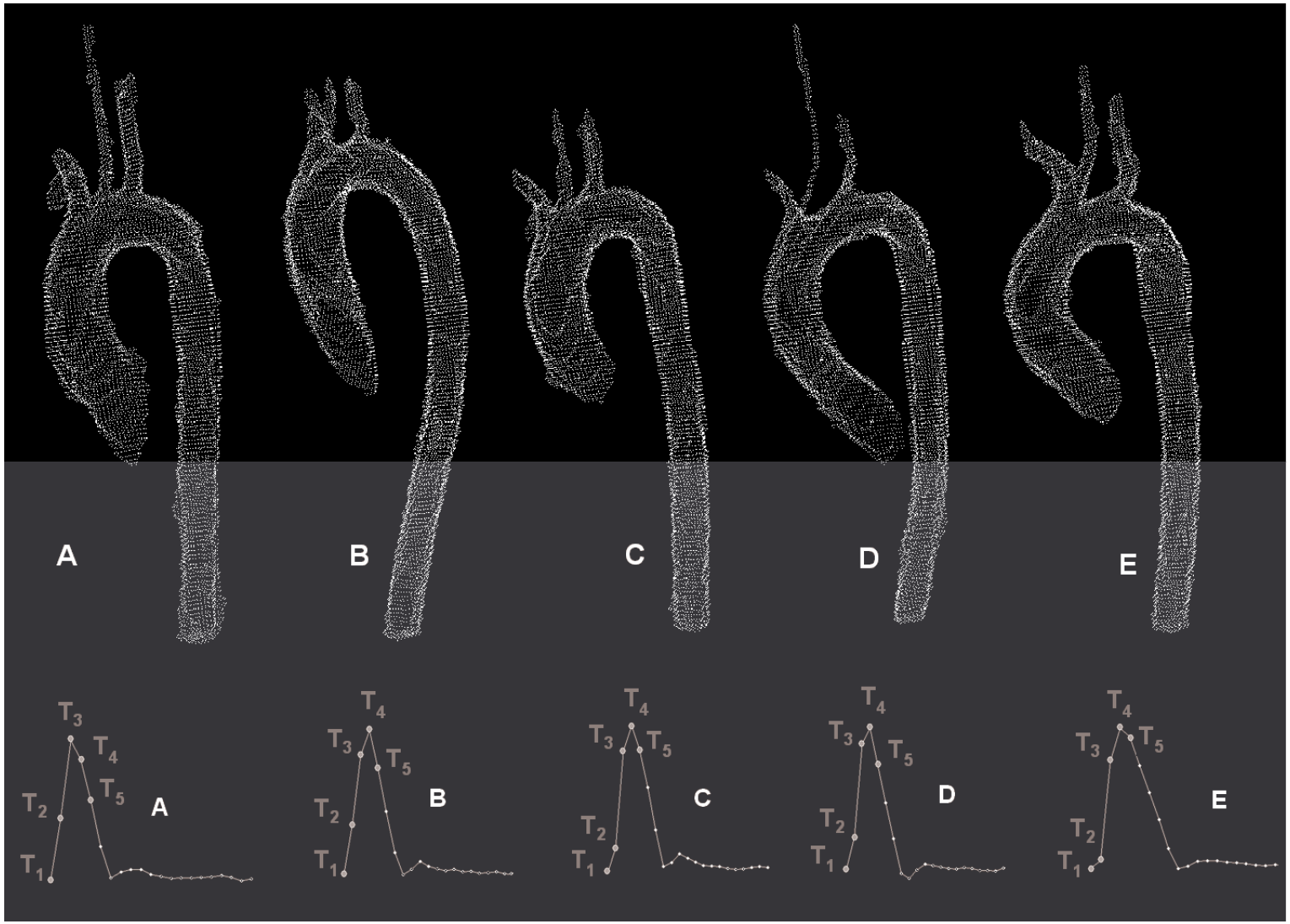

4D Evolution of the Aortic Flow – Lagrangian Analysis

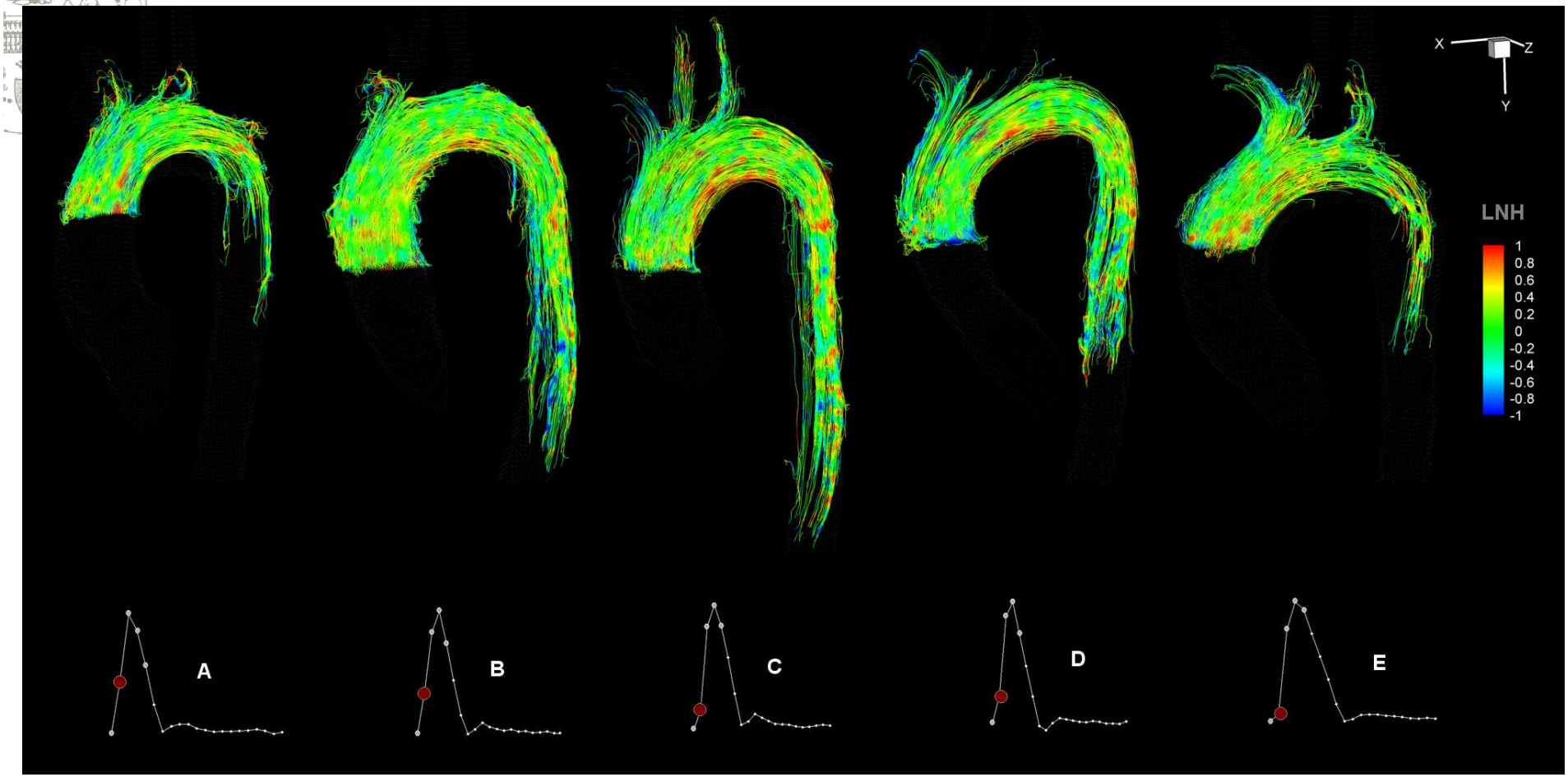

Evolution of particles sets emitted at early systole
Blood is conveyed into the aorta with streaming patterns aligned with the aortic axis: no formation of evident helical vortices can be appreciated

4D Evolution of the Aortic Flow – Lagrangian Analysis

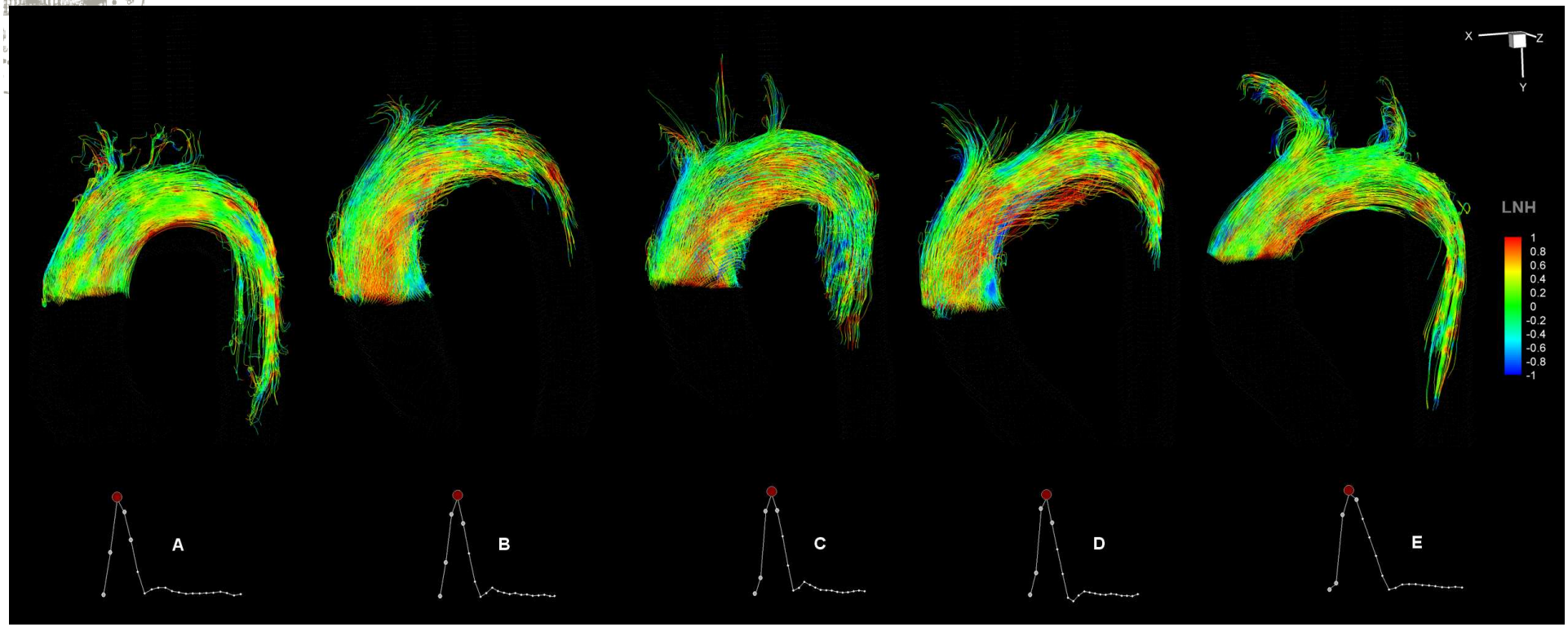

Evolution of the particle set emitted after peak systole is strongly characterized by the onset of more coherent helical structures

4D Evolution of the Aortic Flow – SUBJECT C

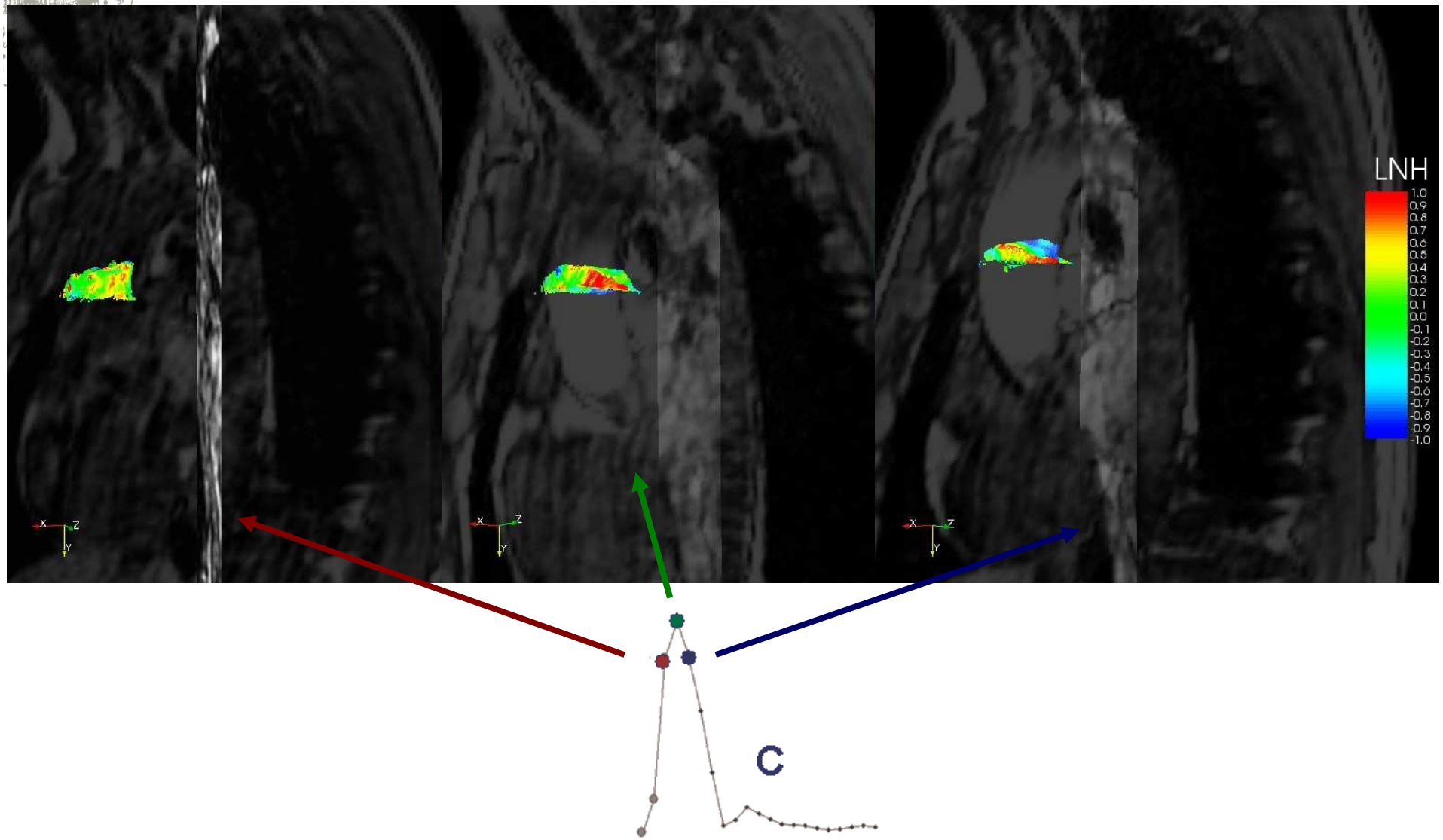

4D Evolution of the Aortic Flow – SUBJECT E

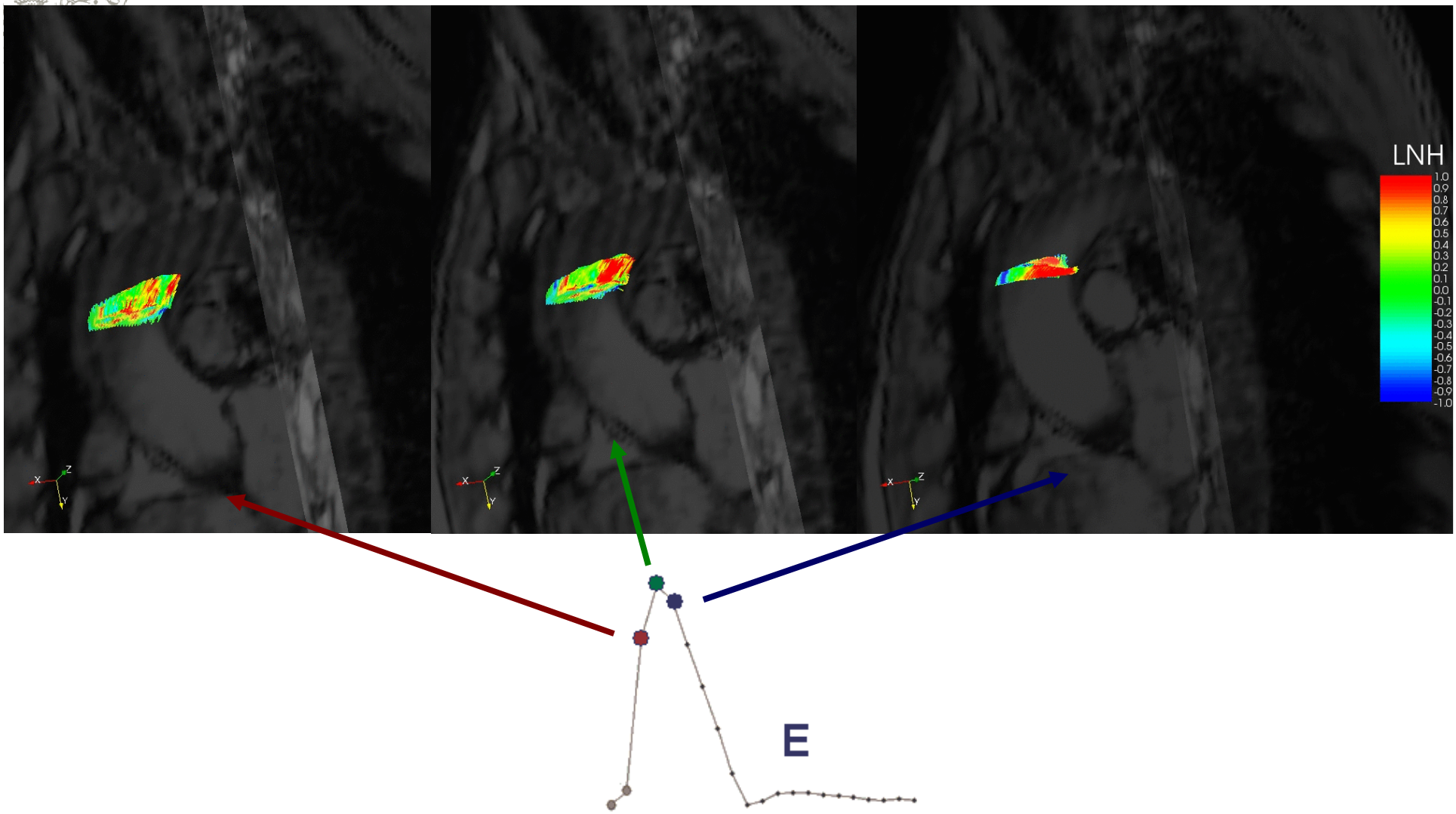

4D Evolution of the Aortic Fl

The flow deceleration phase is dominated by the fluid rotational momentum, resulting in coherent helical and bihelical patterns appearing in the ascending aorta.

The onset of helical patterns in the ascending aorta in the second half of the systole can be better appreciated displaying the first 25 ms of motion of particle sets.

Image is oriented as if observer is looking inferiorly.

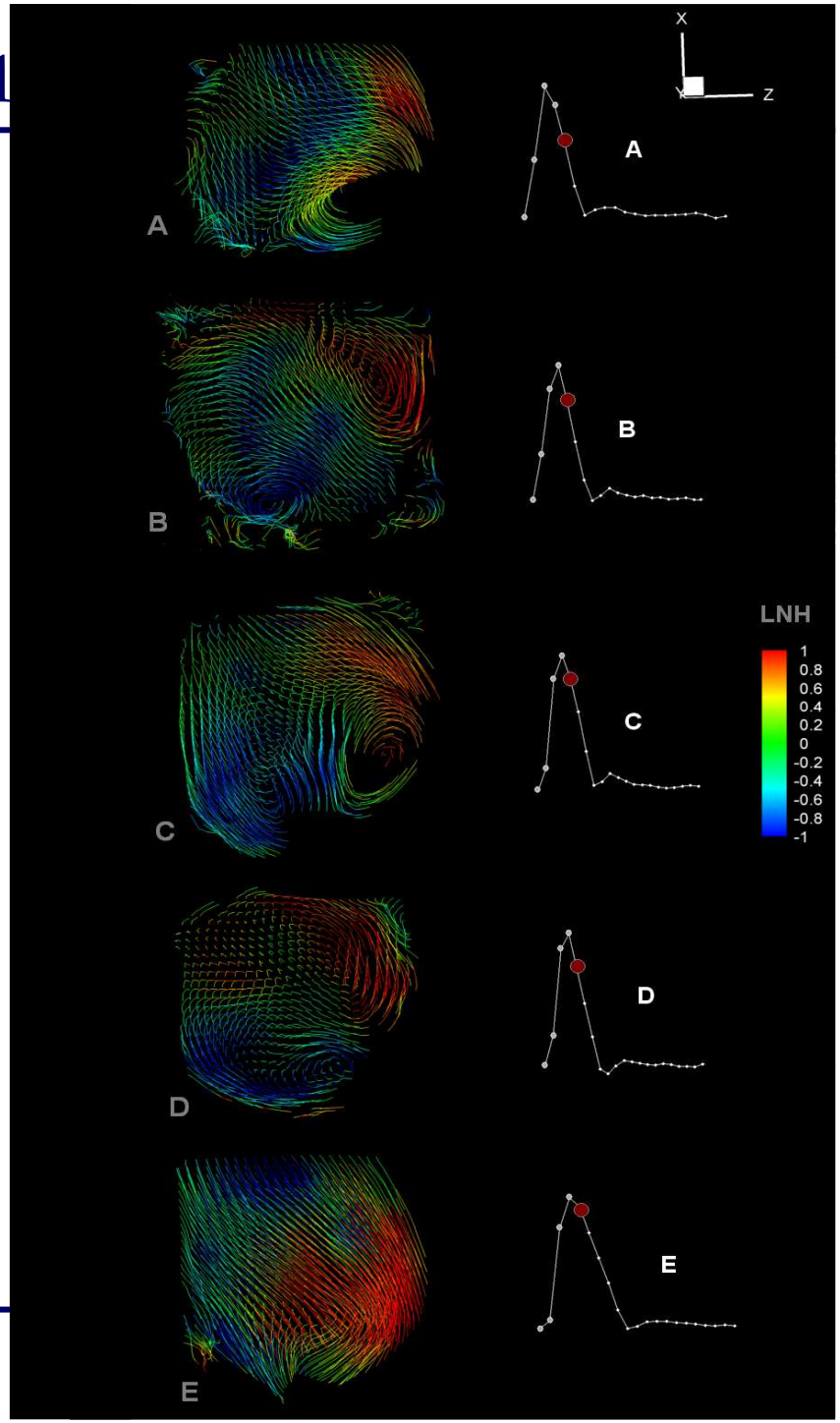

Helical Flow – Quantitative Analysis I

INTRAINDIVIDUAL ANALYSIS

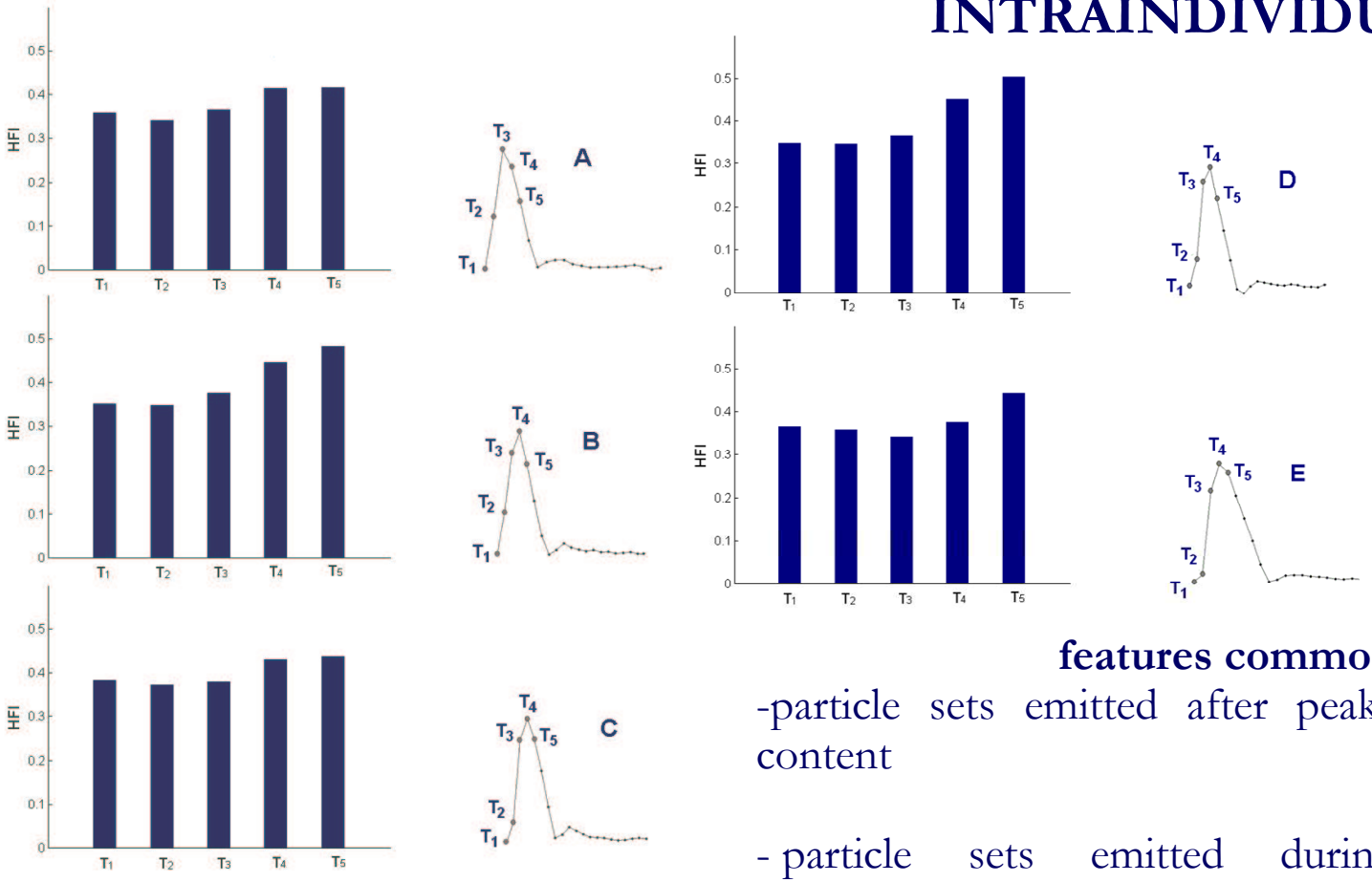

features common to all:

-particle sets emitted after peak-systole, highest helical content

- particle sets emitted during acceleration phase characterized by similar trends in HFI values

bulk flow helical content depends upon the evolution of the flow through the aorta

Helical Flow – Quantitative Analysis III

INTERINDIVIDUAL ANALYSIS

mean HFI values

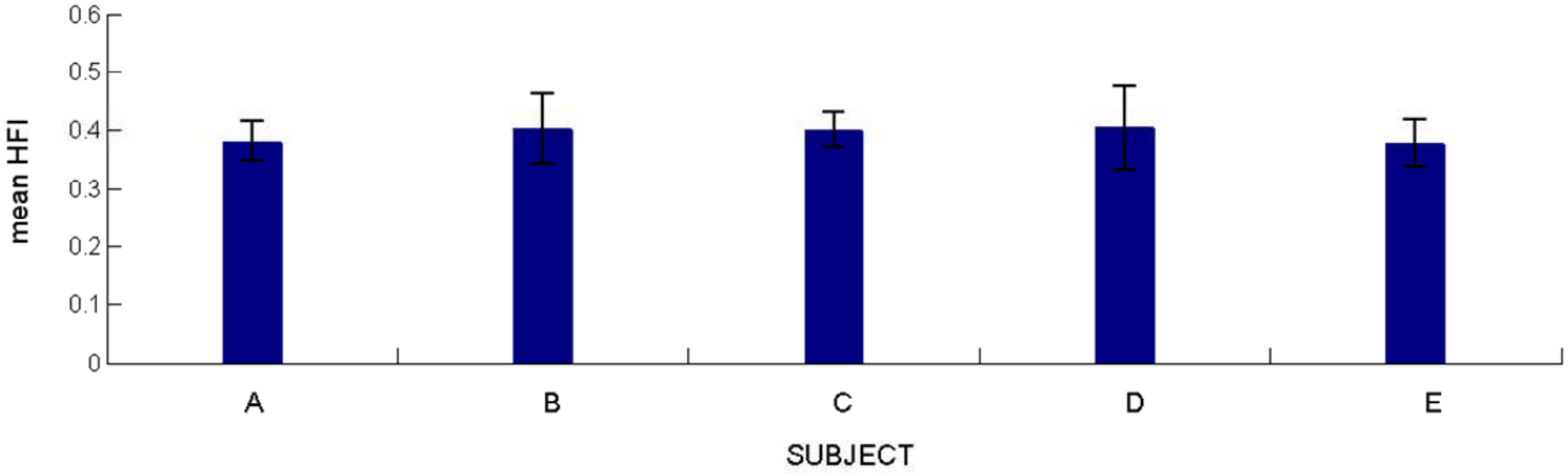

very similar values of mean HFI

healthy individuals exhibit characteristic average systolic content of helical blood flow in aorta

Conclusion

There were two key findings of our study:

(i) intra-individual analysis revealed a statistically significant difference in the helical content at different phases of systole

(ii) group analysis suggested that aortic helical blood flow dynamics is an emerging behavior that is common to healthy individuals

The science applied to assess helical blood flow in vivo could be helpful to raise to still unanswered questions concerning the primary circulation.

Its ability in ranking fluid dynamical behaviour candidates HFI for diagnostic use in clinical practice.

Our results enforce the hypothesis that helicity contribute to **optimize the naturally occurring fluid transport processes in the cardiovascular system, aiming at obtaining an efficient perfusion, avoiding excessive energy dissipation in the process of conveying blood flow in aorta**






umberto.morbiducci@polito.it

On the Use of In Vivo Measured Flow Rates as Boundary Conditions for Image-Based Hemodynamic Models of the Human Aorta. Implications for Indicators of Abnormal Flow

D. Gallo, G. De Santis, F. Negri, D. Tresoldi, R. Ponzini, D. Massai, M.A. Deriu, P. Segers, B. Verhegghe, G. Rizzo

Politecnico di Torino, Italy

CILEA, Italy

IBiTech-bioMMeda, Ghent University, Belgium

IBFM CNR, Italy

Rationale

Flow induced wall shear stress (WSS) is thought to play an important role in the initiation and progression of vascular diseases.
Accurate assessment of WSS in aorta is of paramount importance in order to get further insight into the comprehension of the role played by WSS in vascular disease.

However, while in vivo direct measurements of blood velocities in the bulk and flow rates in aorta are sufficiently affordable and accurate, reliable in vivo estimation of WSS is still a challenge.

Coupling medical imaging and CFD allows to calculate highly resolved blood flow patterns in anatomically realistic models of the thoracic aorta, thus obtaining the distributions of WSS at the luminal surface.

However, **the increasing reliance on CFD for hemodynamic simulations requires a close look at the various assumptions required by the modeling activity.**

In particular, much effort has been spent in the past to assess the sensitivity to **assumptions regarding boundary conditions (BCs).**

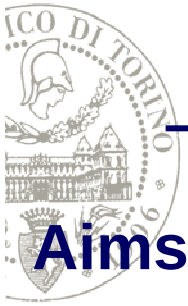

Rationale, Aims, How

Aims

(1) to identify the individual, not invasively measured PC MRI-based BCs scheme that better **replicates** the measured flow rate waveforms;

(2) to describe the **impact that different strategies** of combining PC MRI-based outlet BCs have **on WSS distribution**. The identification of a proper set of individual not-invasively measured BCs can eliminate potential sources of error and uncertainties in blood flow simulations in the human aorta.

Rationale, Aims, How - Flow Chart

How

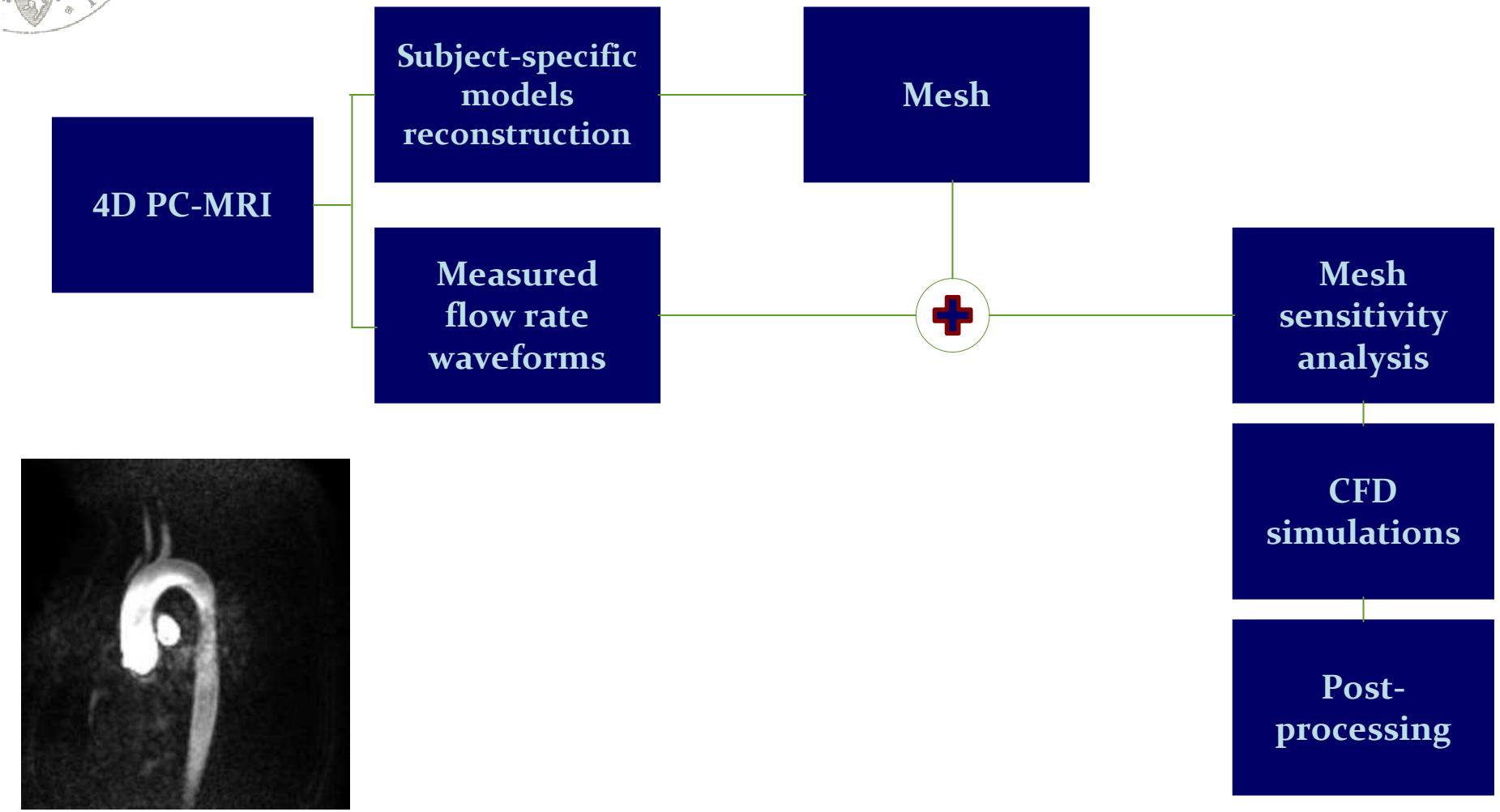

Methods

1) 4D PC-MRI *in-vivo* data → Flow rate waveforms

2) CFD
FINITE VOLUME
(FLUENT SOLVER) →

a) - Navier-Stokes & Continuity

$$\begin{cases} \frac{\partial u}{\partial t} + (u \cdot \nabla)u = -\frac{1}{\rho}\nabla p + \upsilon \Delta u \\ \nabla \cdot u = 0 \end{cases}$$

- blood:

$$\begin{cases} \rho = 1060 \quad kg/m^3 \\ \mu = 0.0035 \quad Pa\,s \end{cases}$$

b) UDF: Boundary Conditions

c) Export WSS on ASCII file

3) MATLAB → Post processing: TAWSS, OSI, RRT

Methods

Fluent Code settings:

- Velocity: second order upwind
- Pressure: linear interpolation
- Pressure –velocity coupling: SIMPLE
- Transient formulation: $\Delta t = 0.001$ ms

Subject-Specific Model Reconstruction

Model A1

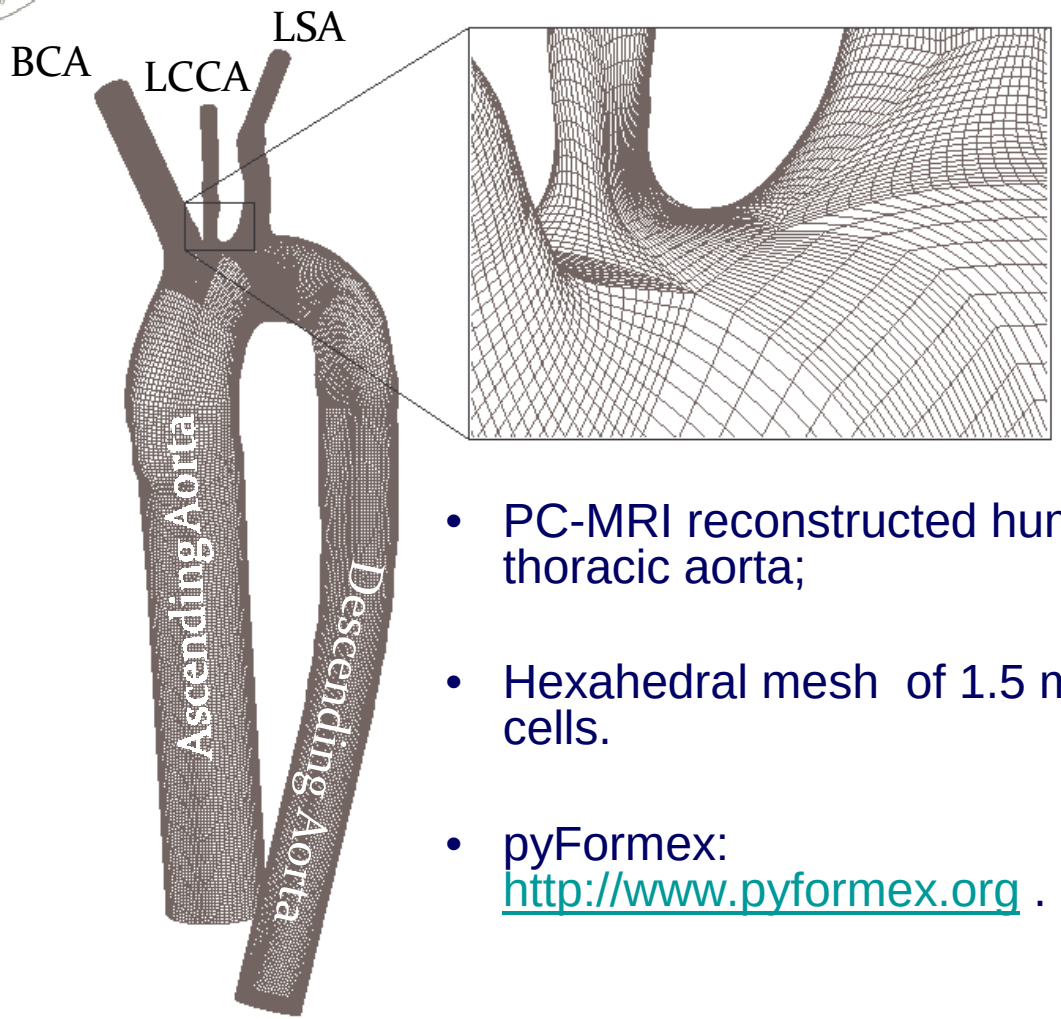

- PC-MRI reconstructed human thoracic aorta;
- Hexahedral mesh of 1.5 million cells.
- pyFormex: http://www.pyformex.org .

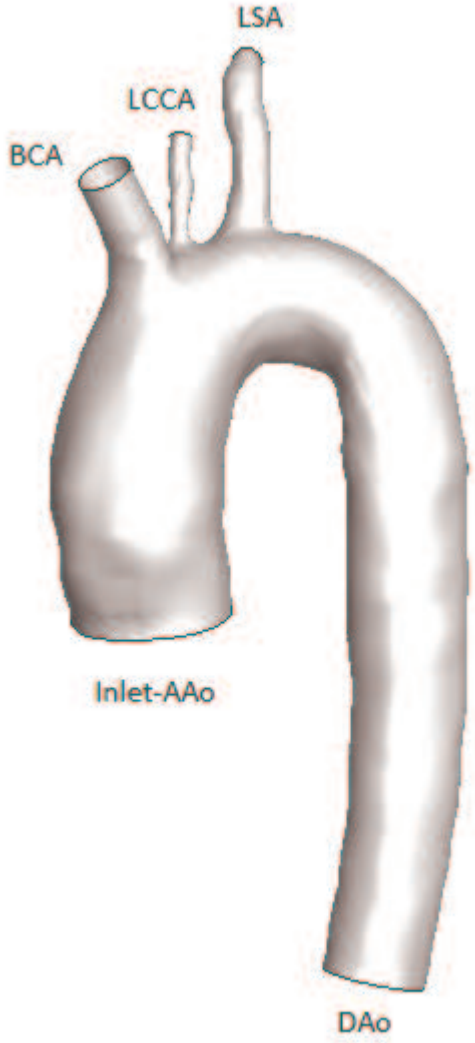

Subject-Specific Model Reconstruction

Model A2

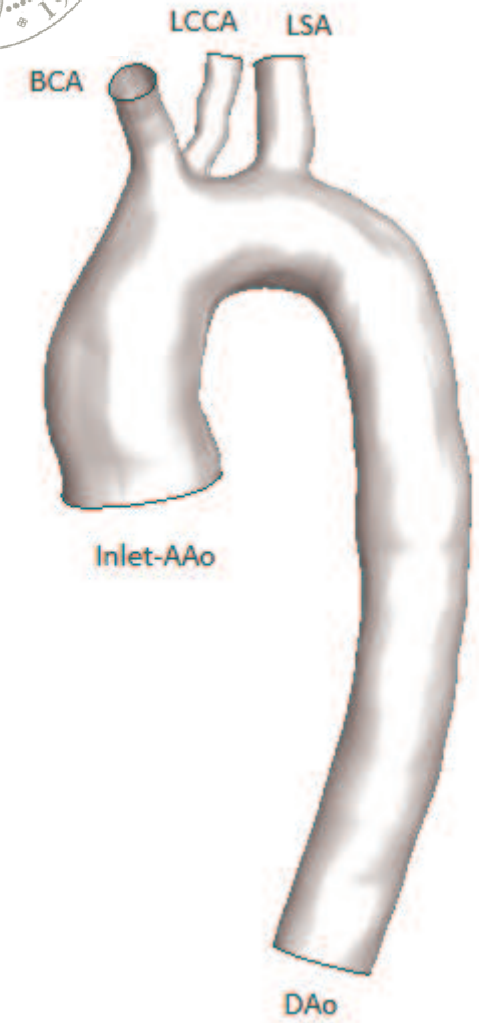

- PC-MRI reconstructed human thoracic aorta;
- Hexahedral mesh of 1.5 million cells.
- pyFormex: http://www.pyformex.org .

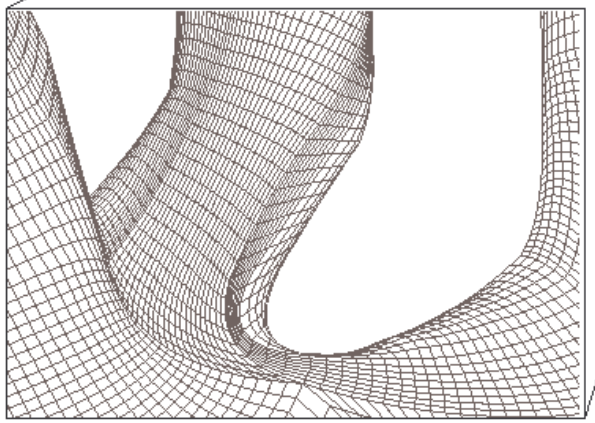

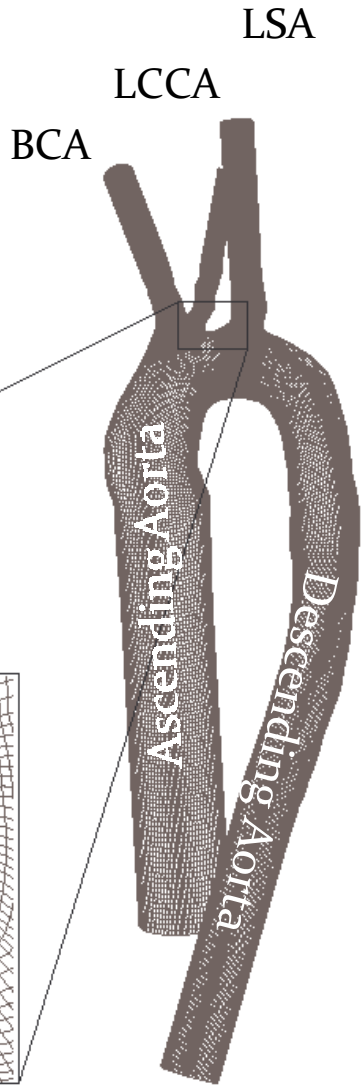

Measured Flow Rate Waveforms

Measured Flow Rate Waveforms as Boundary Conditions in Hemodynamic Simulations

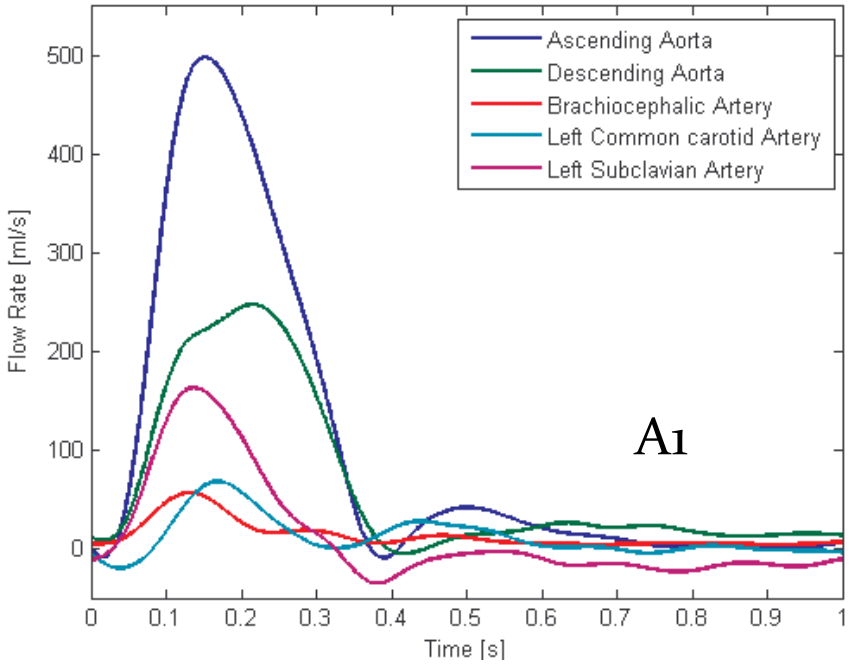

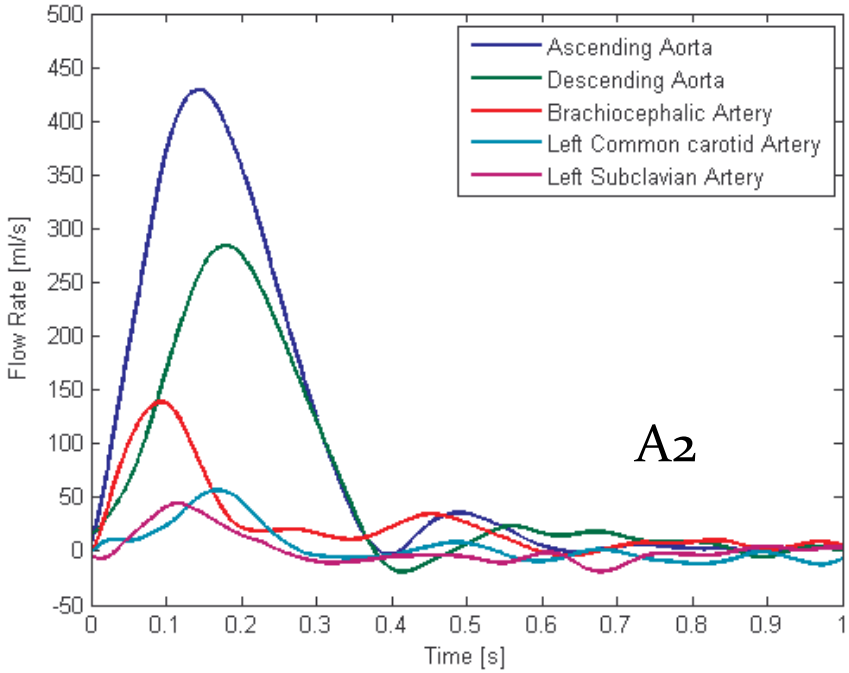

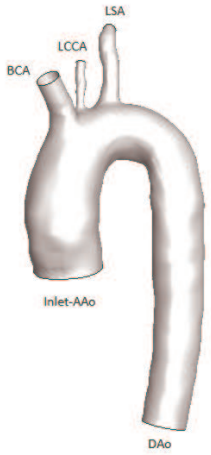

AAO – ascending aorta

Dao – descending aorta

BCA – brachiocephalic artery

LCCA – left common carotid artery

LSA – left subclavian artery

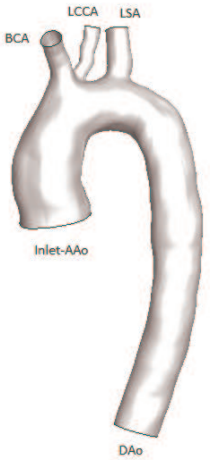

Boundary Conditions

P: **Stress free condition**
COR: **Constant Outflow Ratio (% of AAo inlet flow rate)**
MFR: **Measured Flow Rate**

Outlet Treatment Scheme	DAo	BCA	LCCA	LSA
I	P	COR	COR	COR
II	MFR	P	P	P
III	P	P	P	P
IV	MFR	COR	COR	P
V	MFR	MFR	P	P
VI	P	MFR	MFR	MFR

Constant Outflow Ratio	*Model A1*	*Model A2*
BCA	13.4%	26.7%
LCCA	10.6%	5.5%
LSA	12.0%	0.3%

Flow rate at AAo inlet section prescribed in terms of flat velocity profile

WSS-based Descriptors of Abnormal Flow

TAWSS (Time Averaged WSS)

$$TAWSS = \frac{1}{T}\int_0^T |WSS(s,t)|\, dt$$

- TAWSS < 0.4 Pa → **atherogenic risk**
- TAWSS > 1.5 Pa → **atheroprotective**
- TAWSS > 10-15 Pa → **endothelial damage**

WSS-based Descriptors of Abnormal Flow

OSI (Oscillating Shear Index)

$$OSI = 0.5\left[1 - \frac{\left|\int_0^T WSS(s,t)dt\right|}{\int_0^T |WSS(s,t)|dt}\right]$$

- High OSI → **intimal thickening**

WSS-based Descriptors of Abnormal Flow

RRT (Relative Residence Time)

$$RRT = \frac{1}{(1-2OSI)TAWSS} = \frac{T}{\left| \int_0^T WSS(s,t)dt \right|}$$

- High RRT ⟶ **atherosusceptible**
- Low RRT ⟶ **atheroprotective**

Data Reduction Strategy - Patching

TAWSS1: TAWSS < 0.5 Pa
TAWSS2: TAWSS < 0.6 Pa
TAWSS3: TAWSS < 0.7 Pa

OSI1: OSI > 0.2
OSI2: OSI > 0.3
OSI3: OSI > 0.4

RRT1: RRT > 4 m^2/N
RRT2: RRT > 6 m^2/N
RRT3: RRT > 8 m^2/N

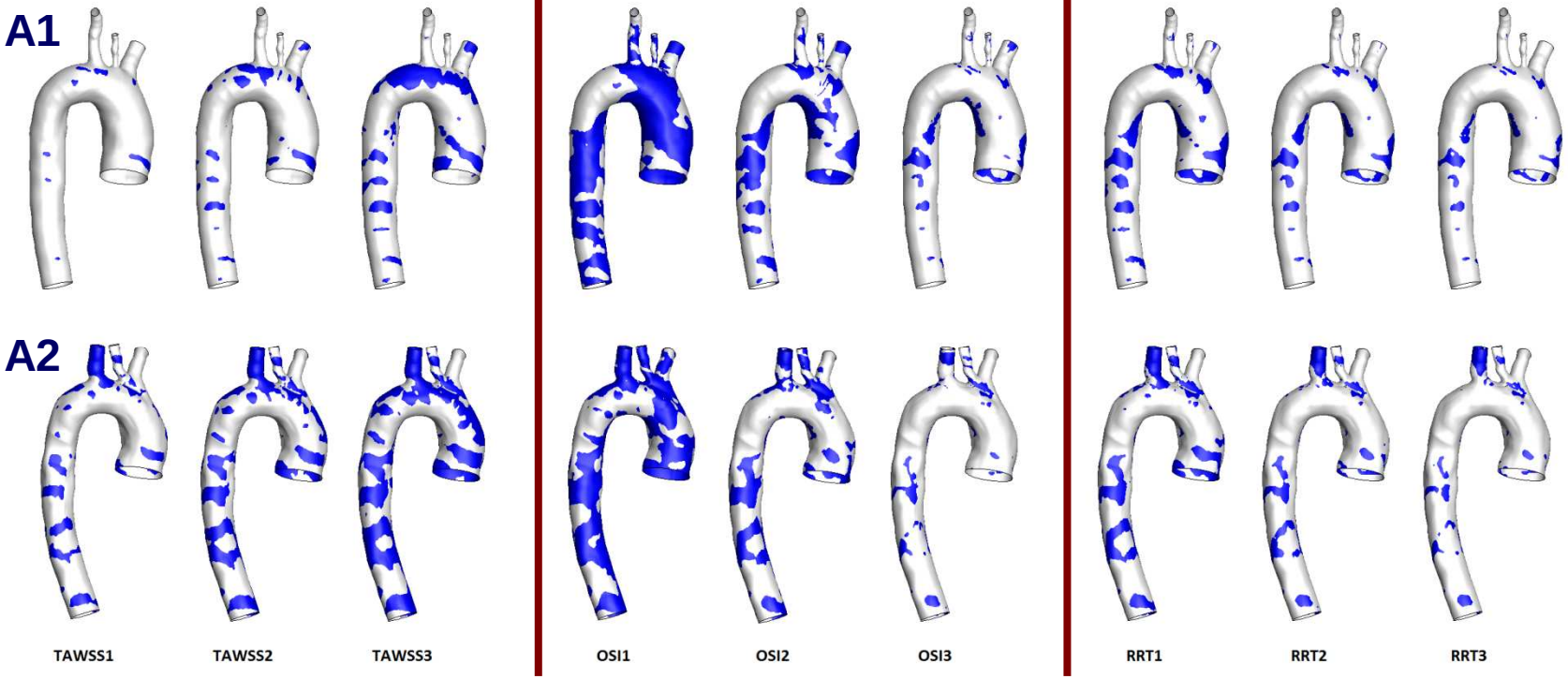

Root Mean Square (RMS) of TAWSS, OSI and RRT was computed over patches.

Data Reduction Strategy – Interindividual Analysis

Aorta models *A1* and *A2* were compared using Cohen distance *d*:

$$d = \frac{\overline{\mu_{A1}} - \overline{\mu_{A2}}}{\sigma_{pooled}} \qquad \sigma_{pooled} = \frac{\overline{\sigma_{A1}} + \overline{\sigma_{A2}}}{2}$$

For a chosen index and a model *Ai*:

- $\overline{\mu_{Ai}}$ is the area-averaged mean of the index;
- $\overline{\sigma_{Ai}}$ is the area-averaged standard deviation of the index.

Mesh Sensitivity Analysis

Aorta A2: 6 refinements 10.000 ÷ 1.500.000;

Distributions of descriptors associated with each grid were compared through Cohen d;

The trend of d indicates that, refining the mesh, the descriptors become closer to the desired resolution.

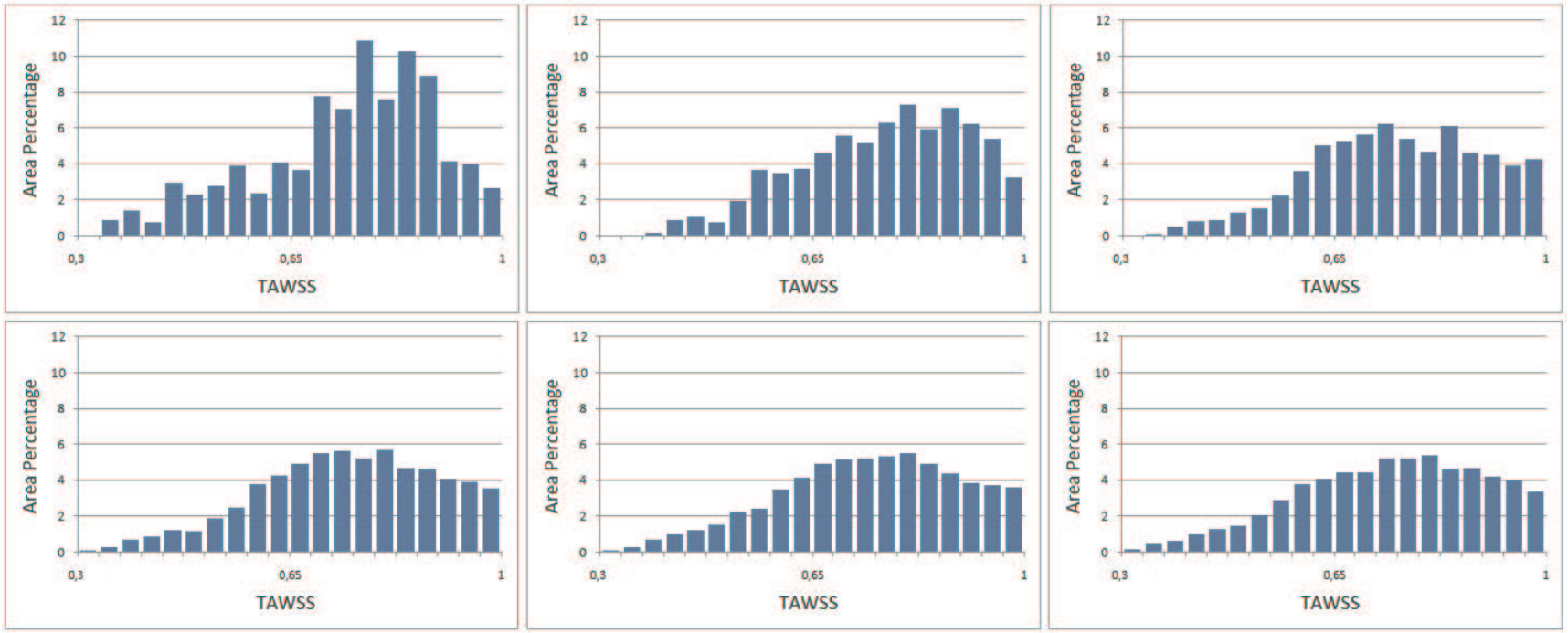

Results – Computed vs Measured Flow Rates

DAO – *in-vivo* vs *in-silico* Flow Rate

scheme I (**blue**) - measured values approximated better for A2

scheme III (**red**) - highest differences

scheme VI (**light blue**) - **agreement with *in-vivo* waveforms**

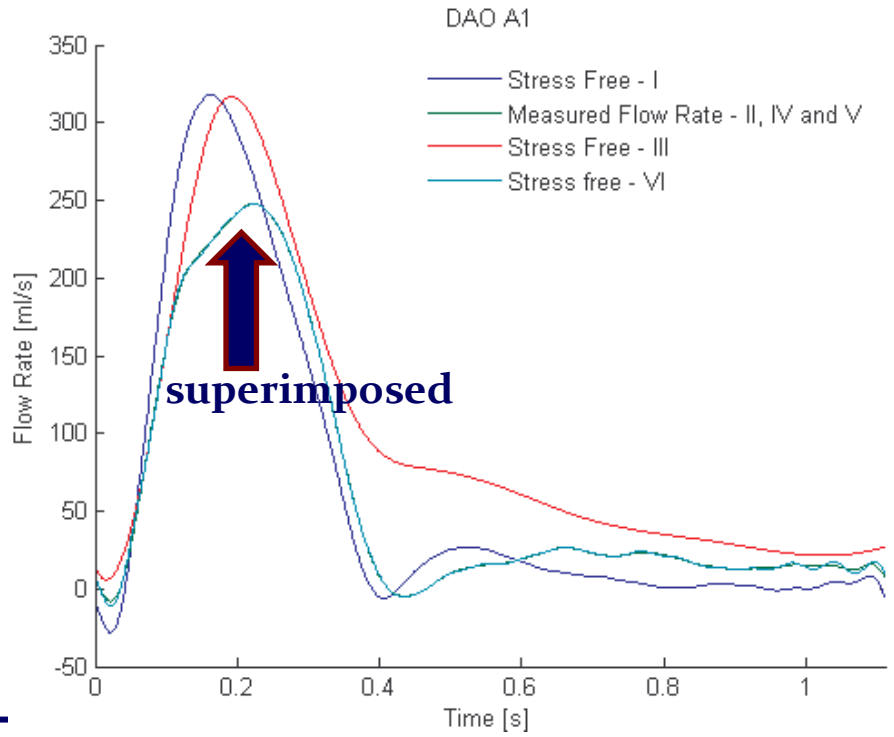

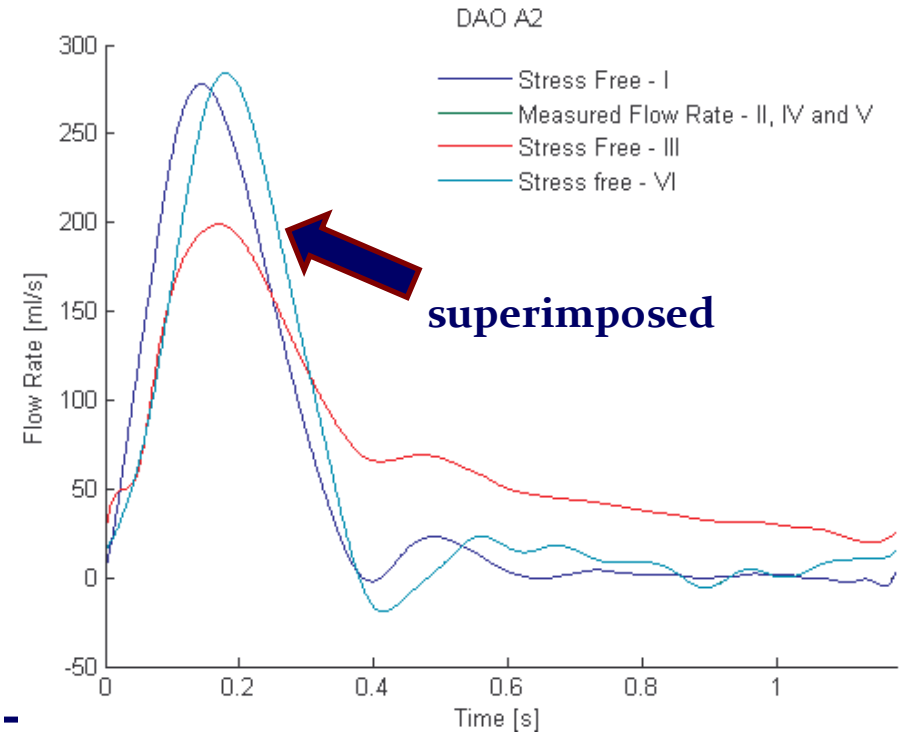

Results – WSS-based Hemodynamic Indicators

TAWSS

Neumann BC on DAo – **P**

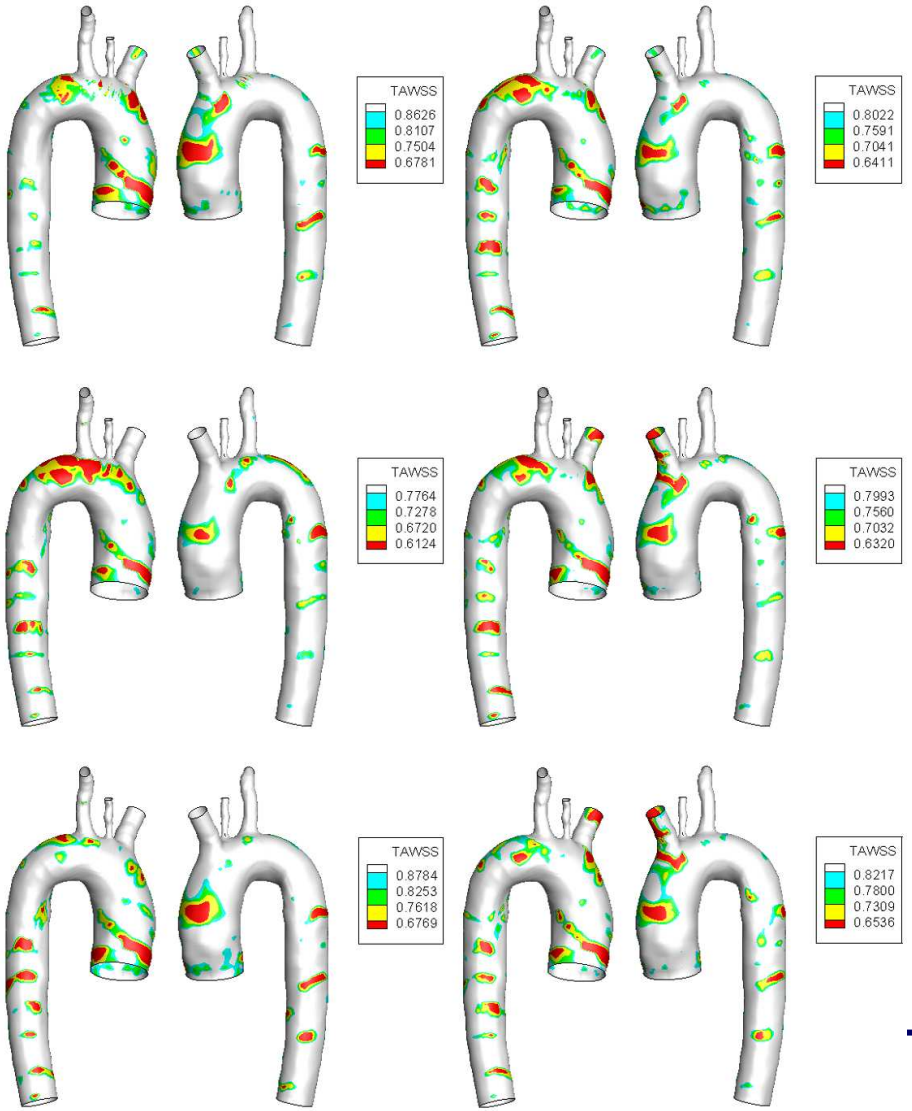

(1) Proximal outer arch curvature

(2) Focal regions on DAo

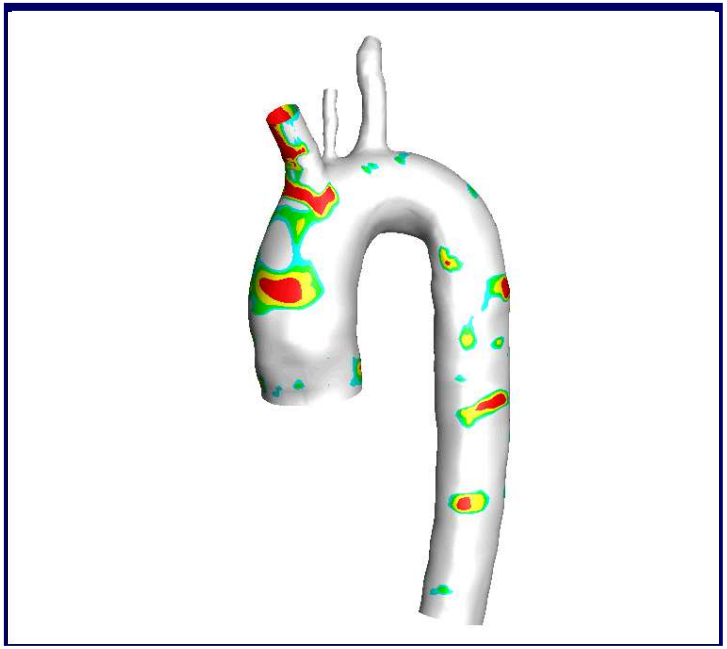

TAWSS VI - Model A1

Results – WSS-based Hemodynamic Indicators

TAWSS

Neumann BC on DAo – **P**

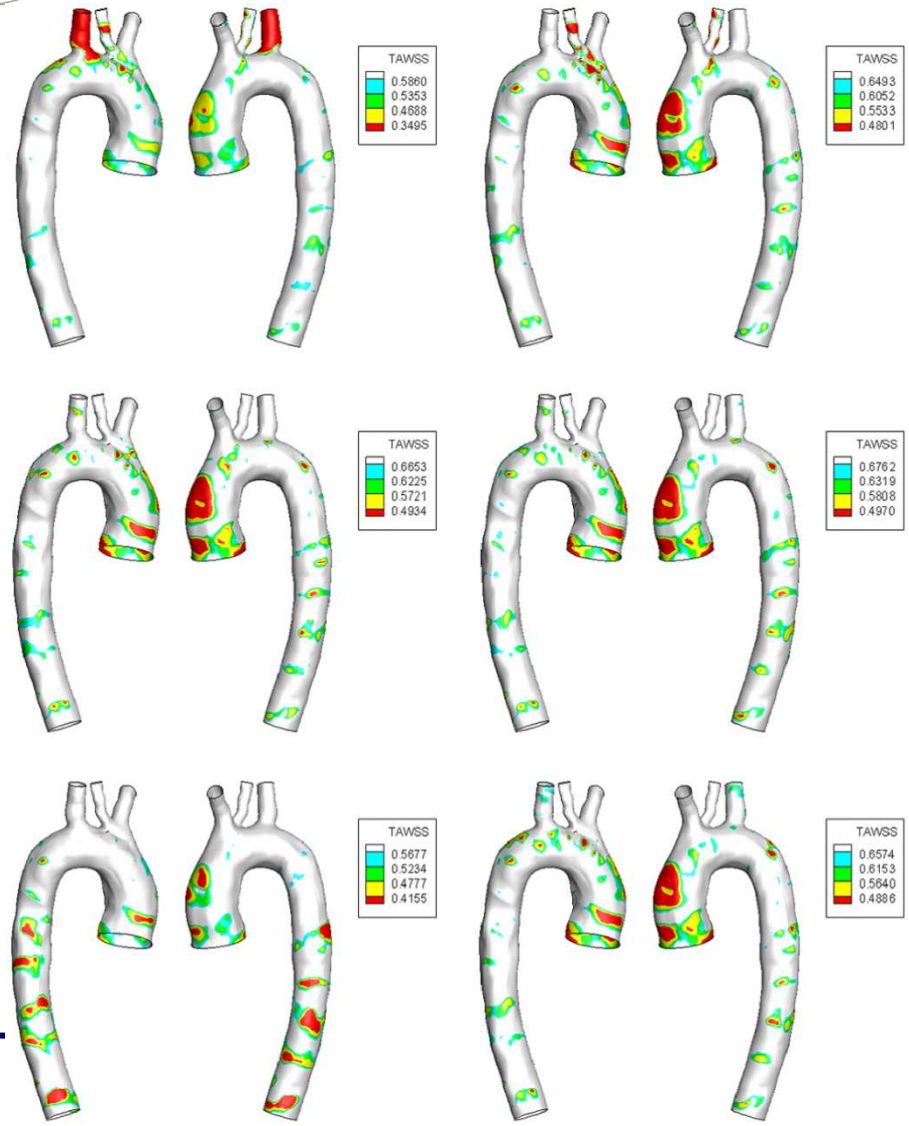

(1) Proximal outer arch curvature

(2) Focal regions on DAo

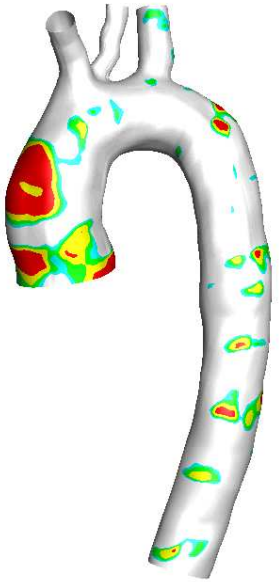

TAWSS VI - Model A2

Results – WSS-based Hemodynamic Indicators

TAWSS

Model A1

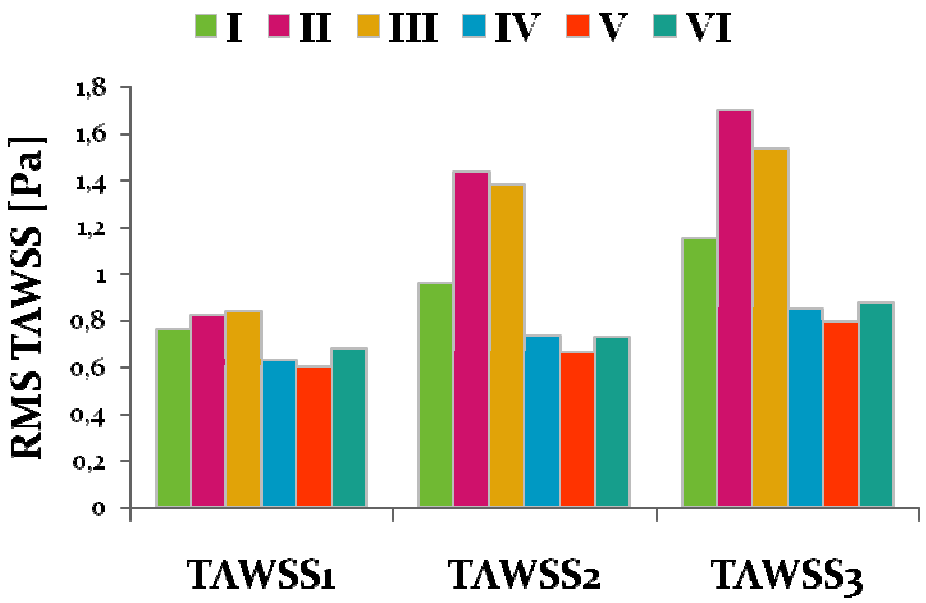

Model A2

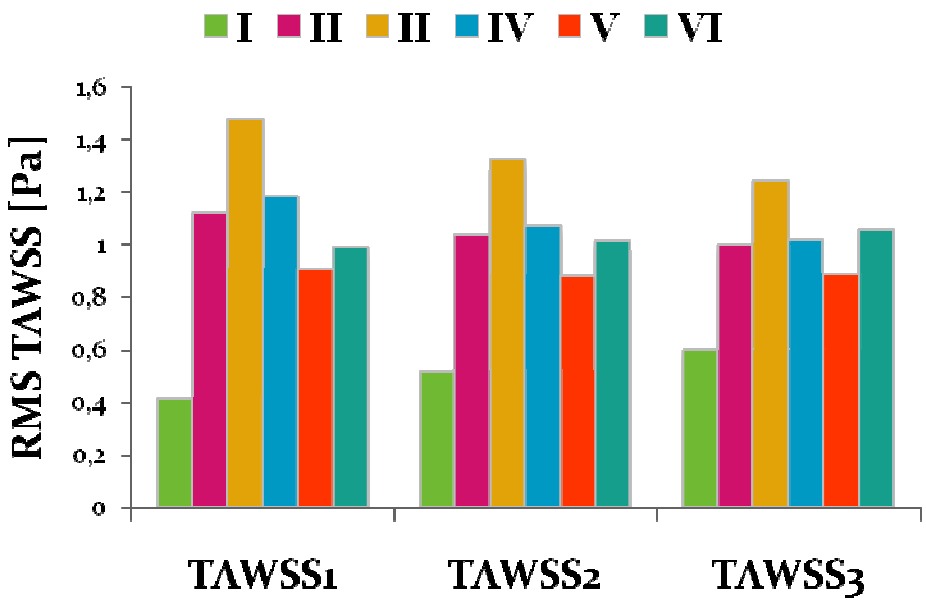

schemes II – III: imposition of stress-free condition at all the supra-aortic sections may reduce flow stagnation regions;

scheme I: on model A2, constant outflow ratio on LSA is 0,3% of the inlet flow at the AAo.

Results – WSS-based Hemodynamic Indicators

Neumann BC on DAo – **P**

OSI

Model A1

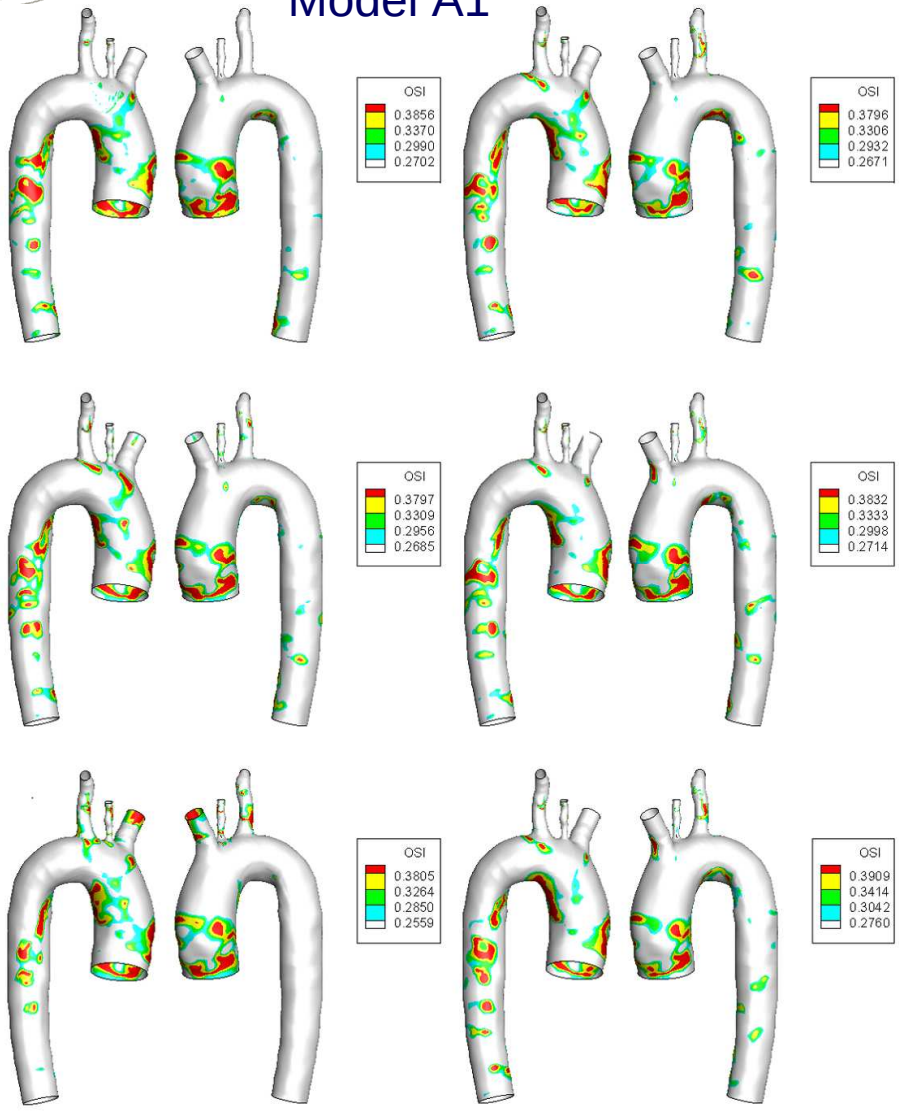

Model A2

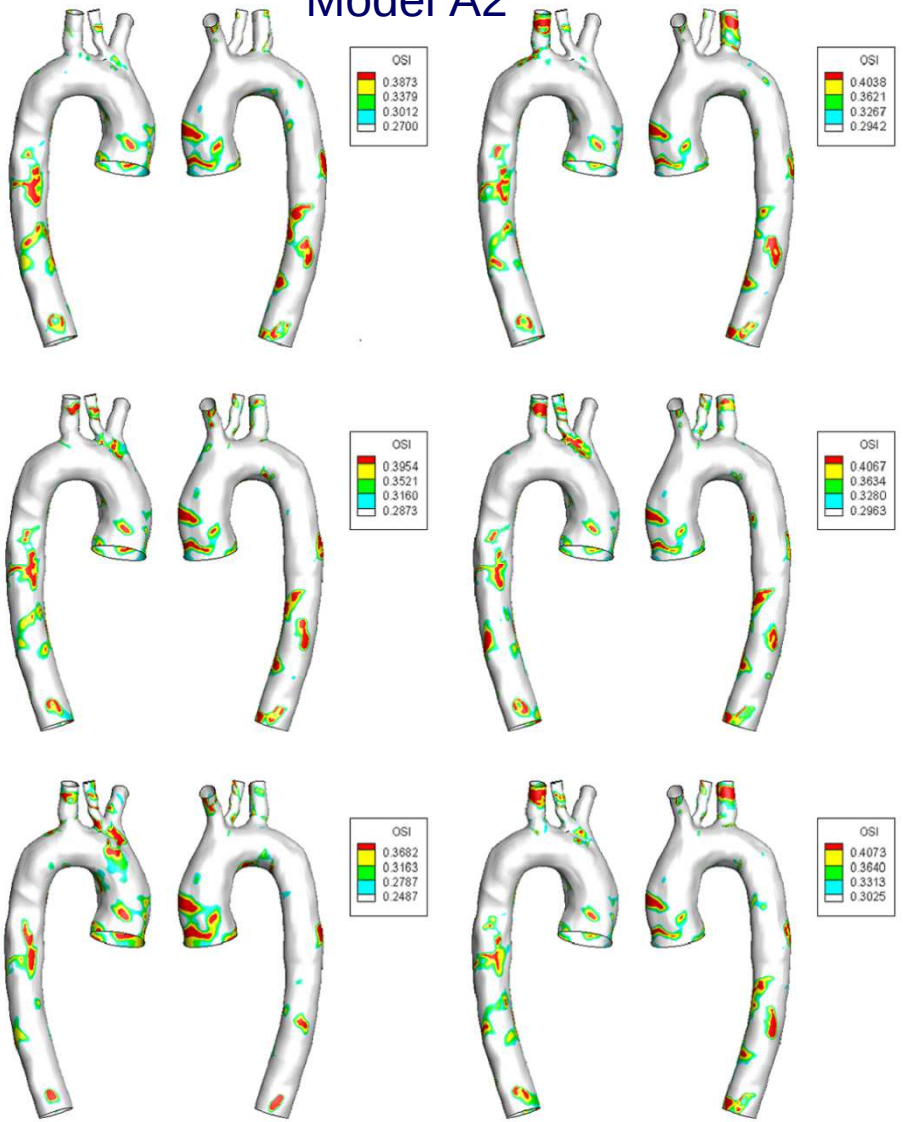

Results – WSS-based Hemodynamic Indicators

OSI

Model A1

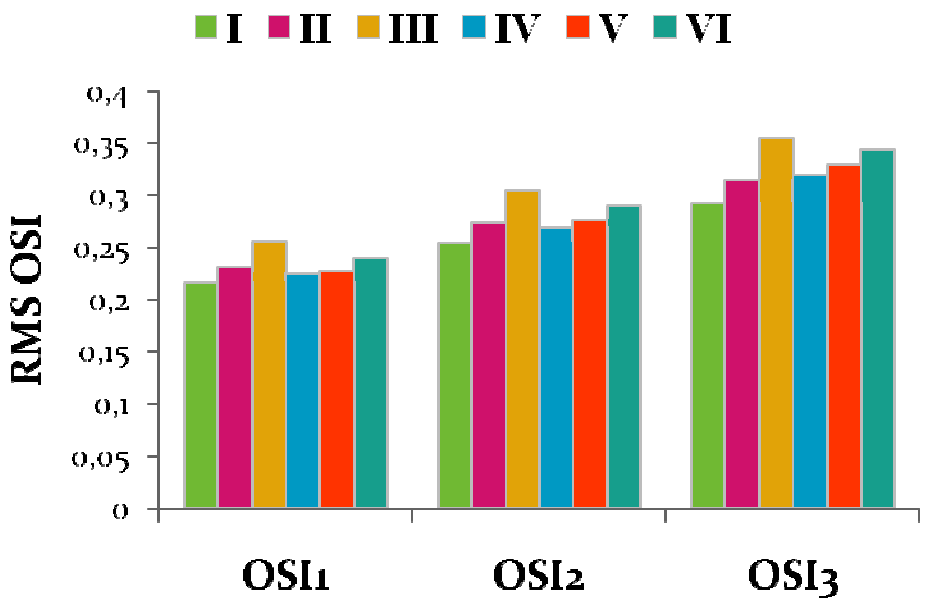

Model A2

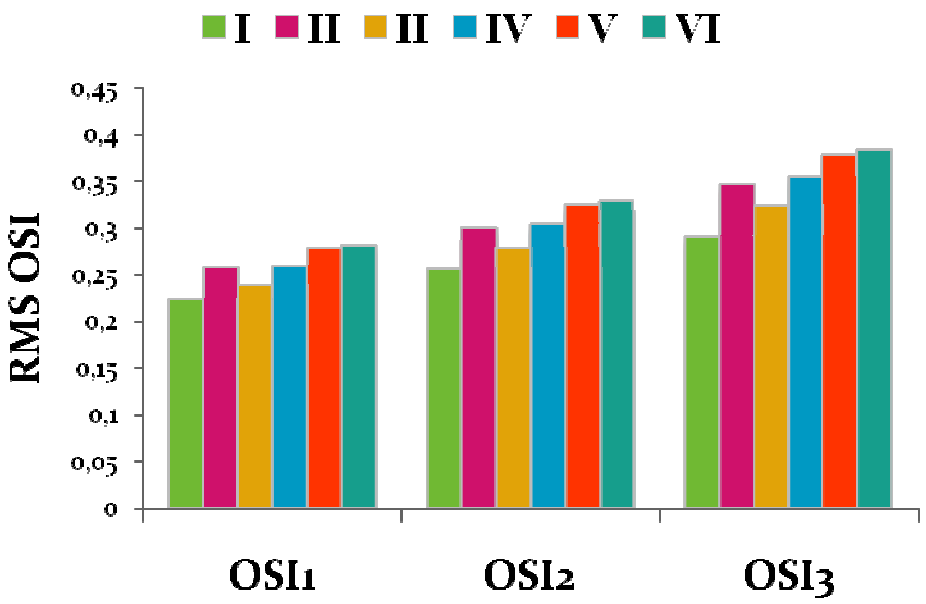

scheme I: low OSI values on both models;

scheme III: on model A2, flow rate waveform of DAo has a damped dynamics with respect to other in-silico and in-vivo flow rate waveforms.

Results – WSS-based Hemodynamic Indicators

Neumann BC on DAo – **P**

RRT

Model A1

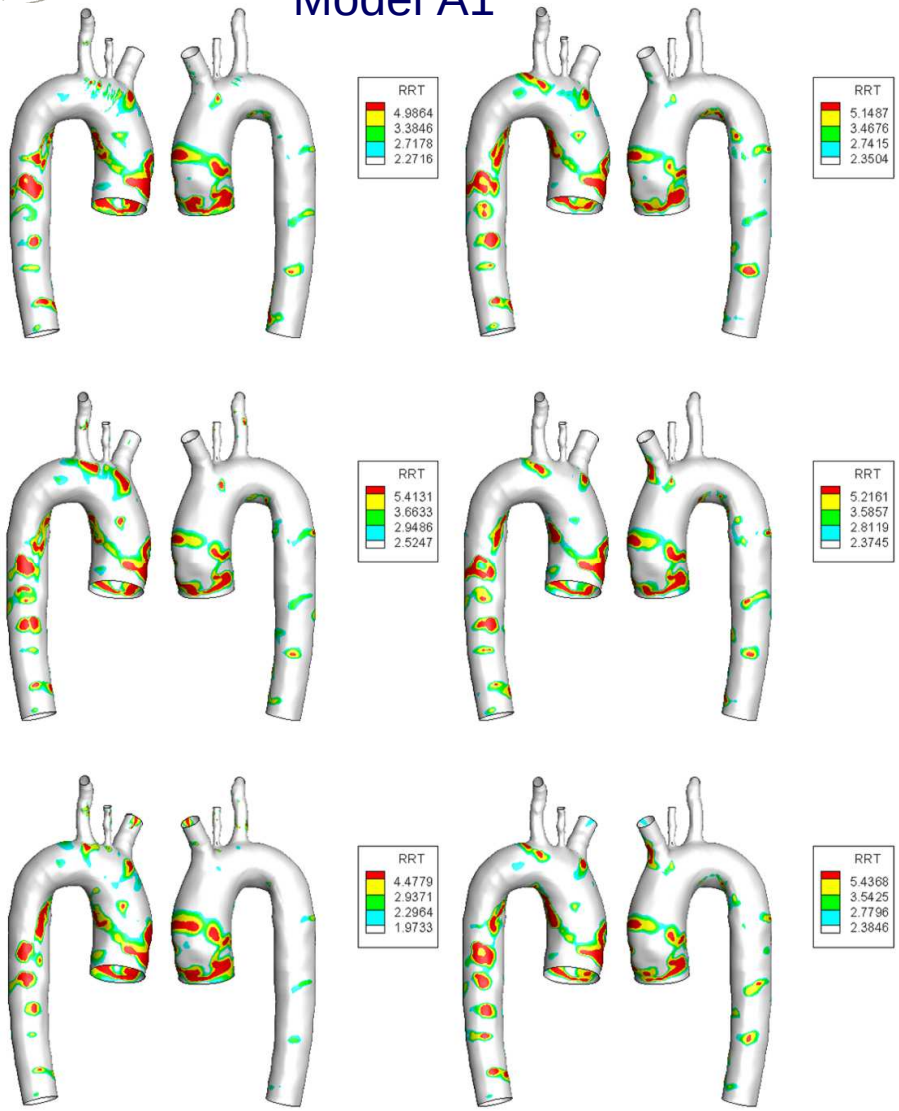

Model A2

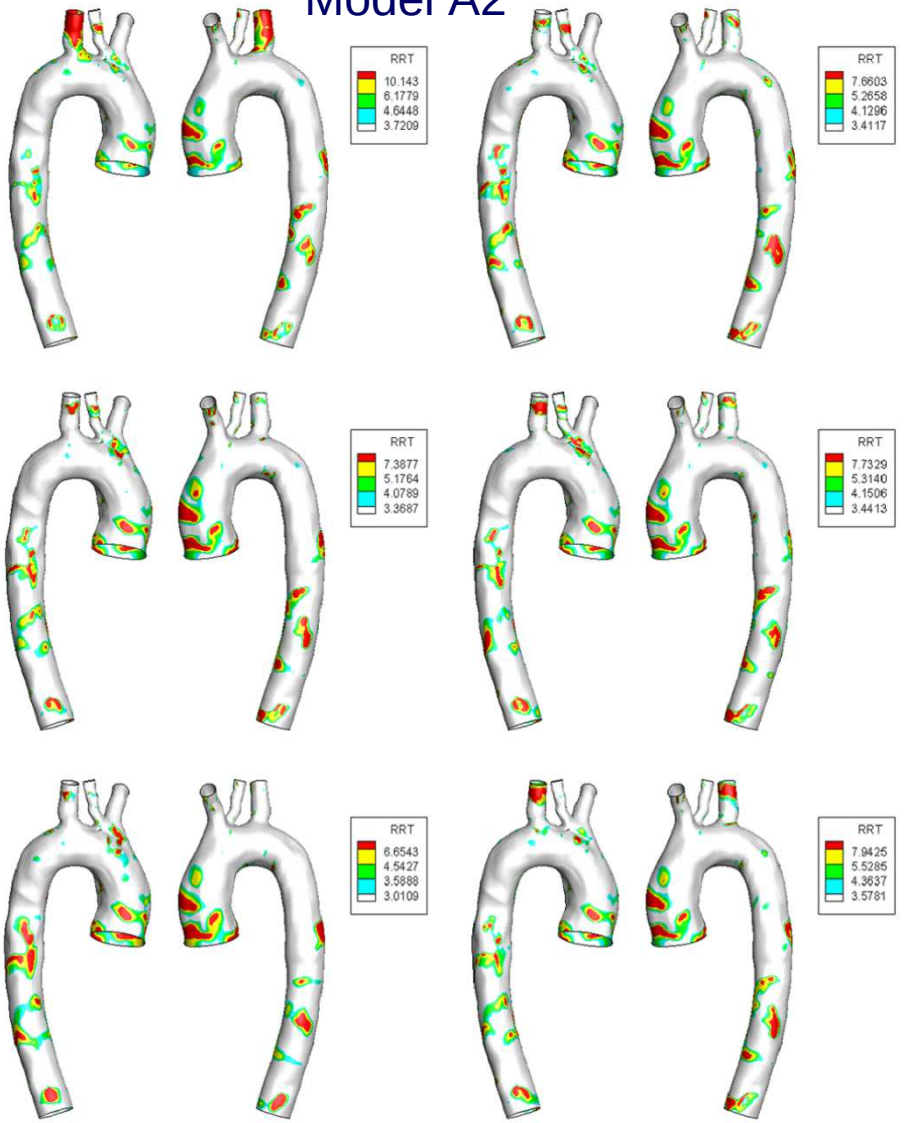

Results – WSS-based Hemodynamic Indicators

RRT

Model A1

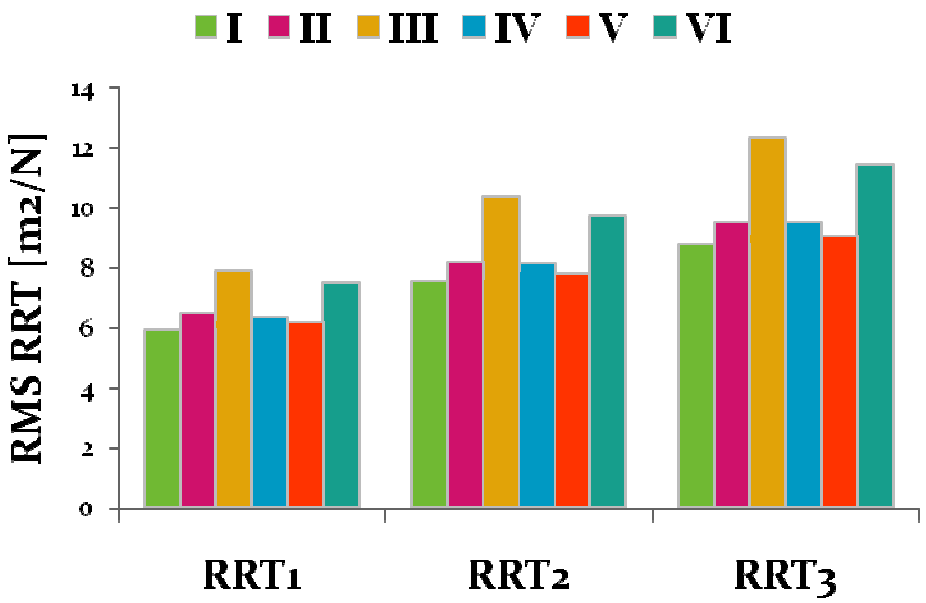

Model A2

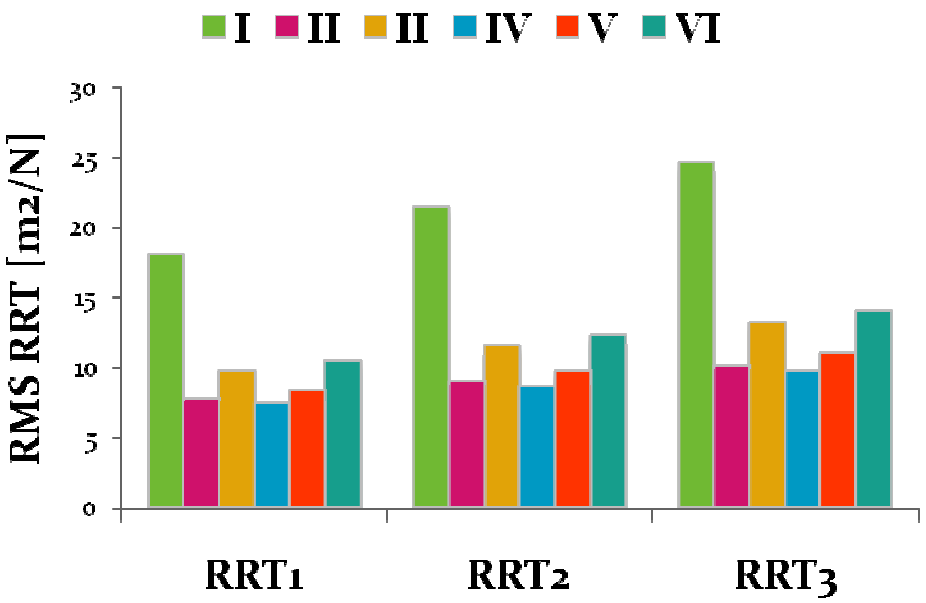

scheme III: high values on model A1, because of high OSI values;

scheme I: high values on model A2, as a consequence of low TAWSS values.

Results – Interindividual Comparison

TAWSS is always higher in model A1 (d > 0);

RRT is always higher in model A2 (d < 0);

OSI *d* has positive or negative signs, depending on the BC scheme;

Model A1 is more atheroresistant.

	BC scheme					
Cohen distance *d*	*I*	*II*	*III*	*IV*	*V*	*VI*
TAWSS	0.3851	0.4246	0.6169	0.3652	0.3724	0.3666
OSI	0.0828	-0.1389	0.0004	-0.1179	-0.2032	-0.1601
RRT	-0.3196	-0.2131	-0.2252	-0.2395	-0.2734	-0.2655

Conclusions

- Patient-specific hemodynamic simulations of aortic flow is feasible by applying scheme VI;

- Prescribing not-invasively measured flow rate as BCs on the supra-aortic branches and pressure on Dao (scheme VI):
  - in-silico blood flow rates match PC-MRI measurements;

- Different schemes of BCs can influence WSS-based descriptors:
  - they mainly affect descriptors value than their distribution;

It is recommended to prescribe time-varying outflow BCs based on in-vivo accurate measurements (for example VI).

On the Use of In Vivo 4D Velocity Profiles as Boundary Conditions for Image-Based Hemodynamic Models of the Human Aorta

D. Gallo, G. Rizzo, R. Ponzini

Politecnico di Torino, Italy **CILEA, Italy** **IBFM CNR, Italy**

Rationale, Aims, How

Rationale

Image-based hemodynamic models of cardiovascular districts can be sensitive to **assumptions regarding boundary conditions**

Aim

Evaluate influence that velocity profiles prescribed at the inlet section (AAo) have in hemodynamic models of the human aorta on:

-Bulk flow
-Wall Shear Stress

How

Image-based hemodynamic models of human aorta & PC MRI individual measurements of 3D velocity profiles

Methods

Image-based model aorta

1mesh 6MLN tethrahedral cells

Finite Volume Method (Fluent Solver)

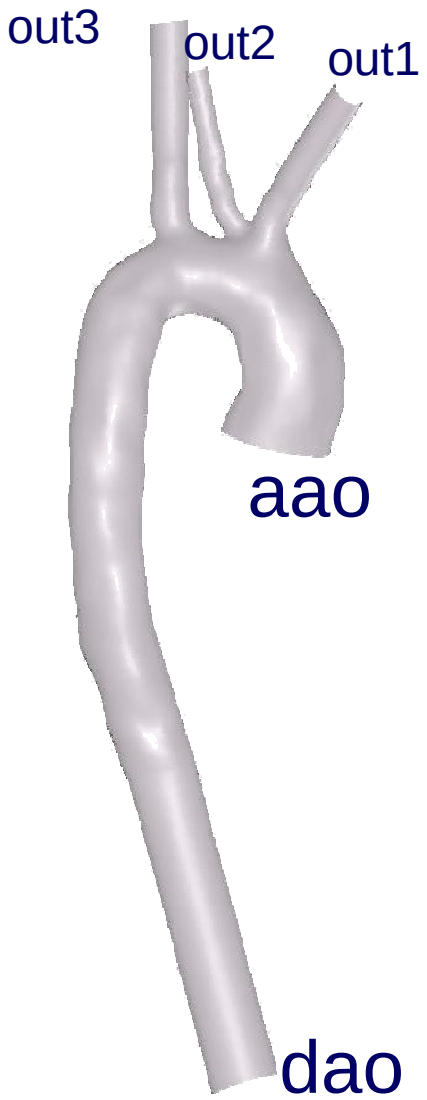

Methods

PRELIMINARY-STUDY

Steady state analysis

2 time frames (T1,T2)

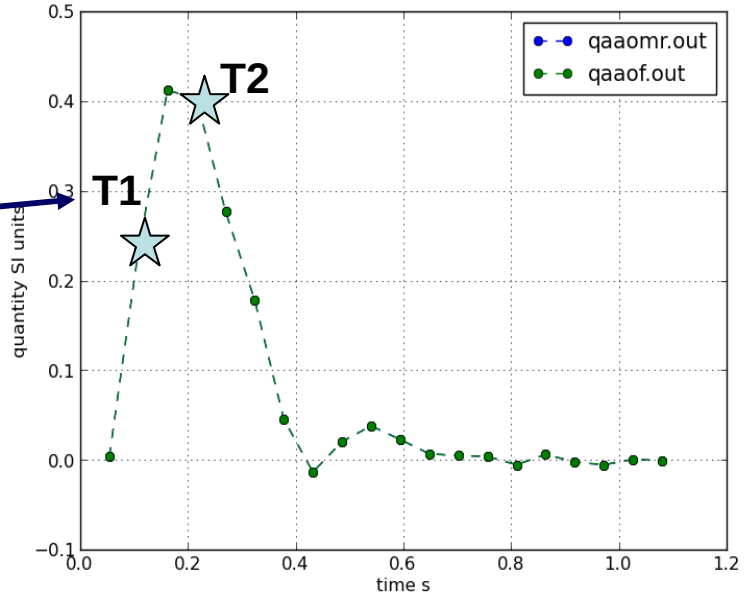

Boundary Conditions

- 3D measured PC MRI Velocity profile
- Flat Velocity profile [V-mean measured (PCMRI)]

Methods – Inlet Boundary Conditions

Inlet section AAo
Velocity vectors

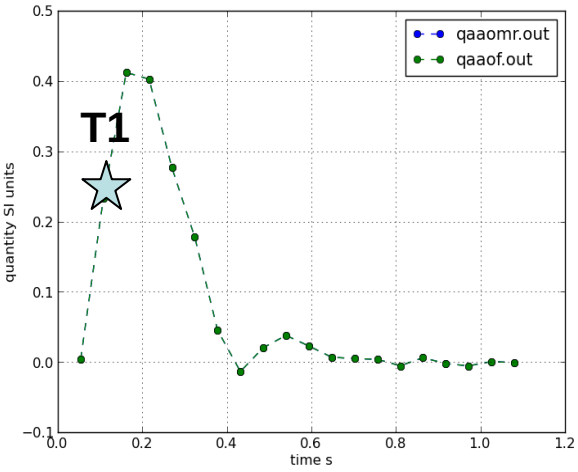

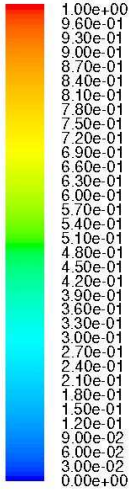

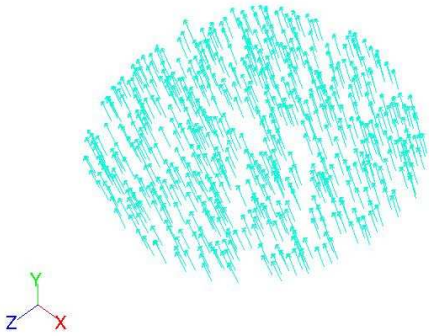

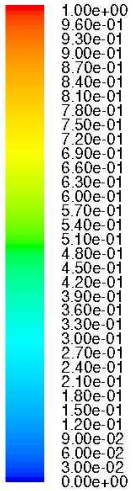

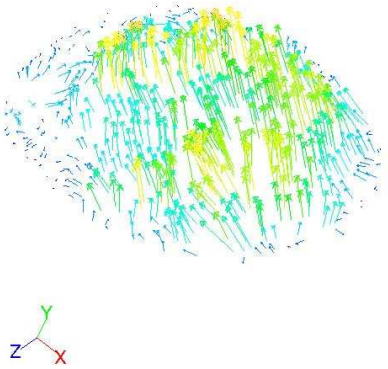

Flat V profile

3D PC MRI
measured profile

Results – Streamlines at T1

Flat V profile

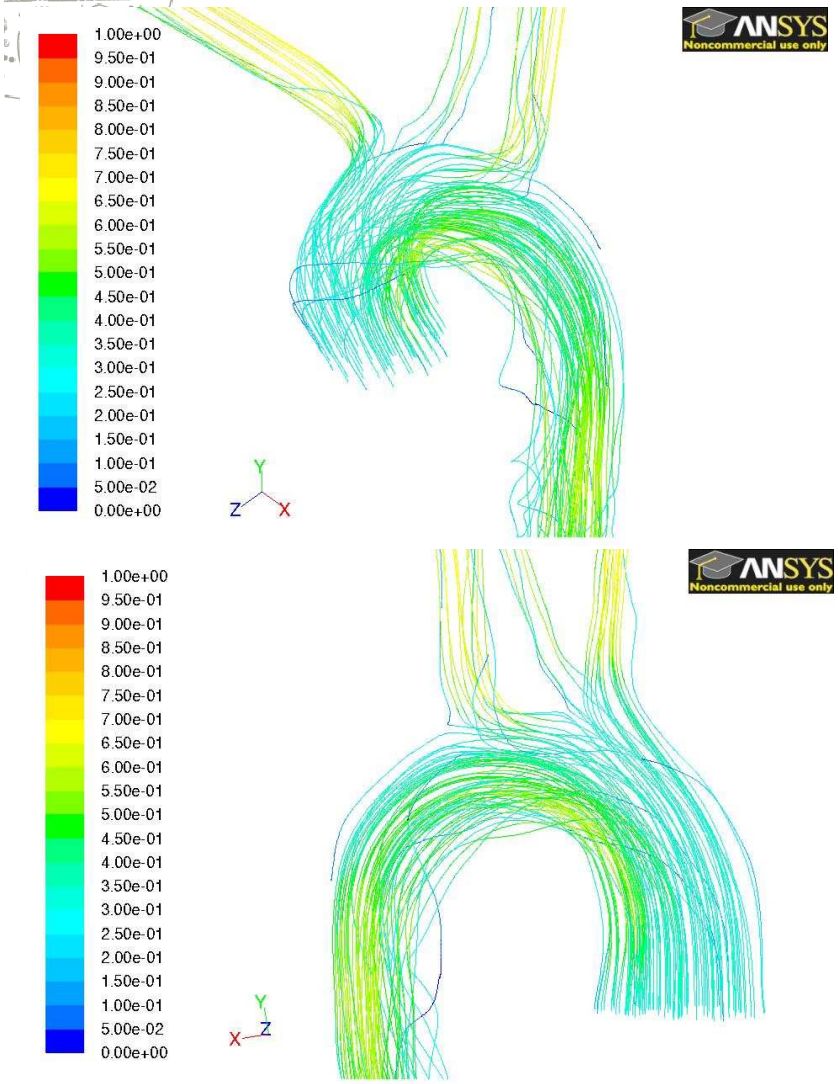

Pathlines Colored by Velocity Magnitude (m/s)

May 03, 2011
ANSYS FLUENT 12.1 (3d, dp, pbns, lam)

3D PC MRI measured profile

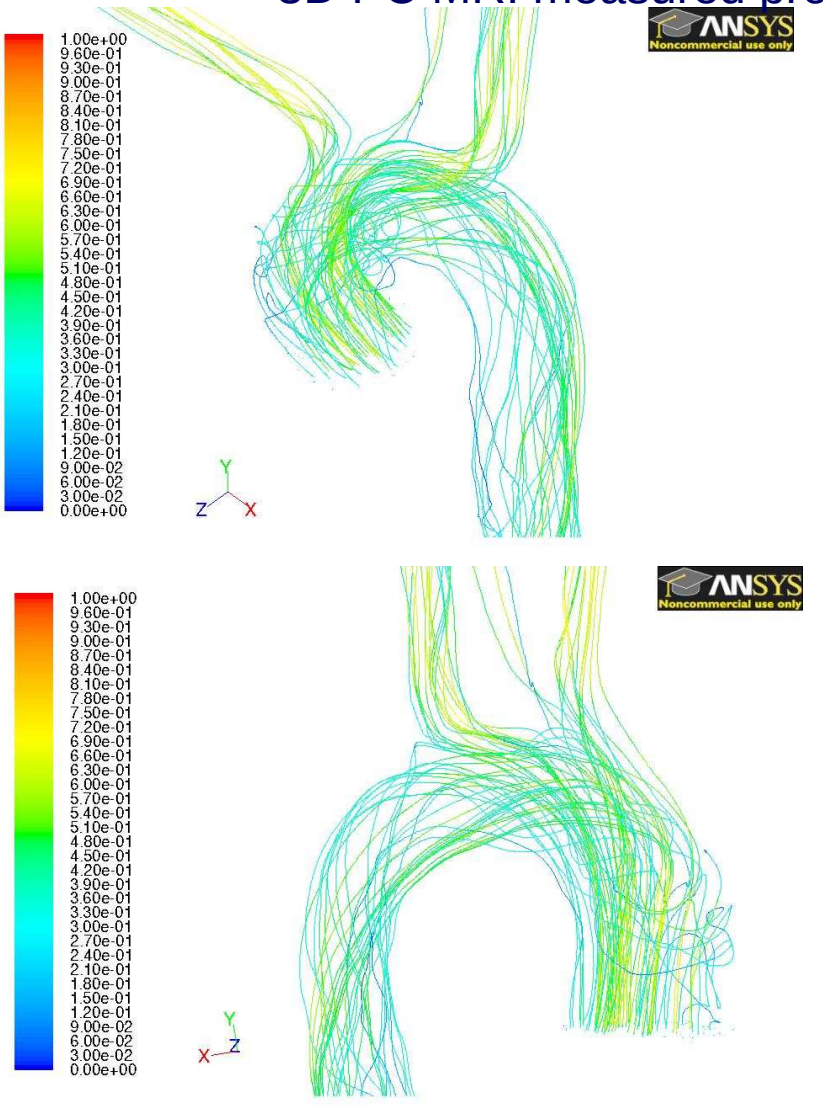

Pathlines Colored by Velocity Magnitude (m/s)

May 03, 2011
ANSYS FLUENT 12.1 (3d, dp, pbns, lam)

Results – WSS at T1

Flat V profile

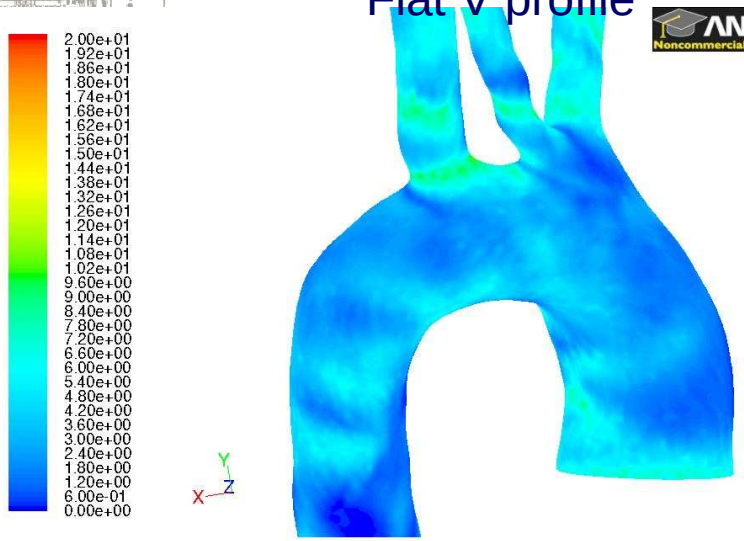

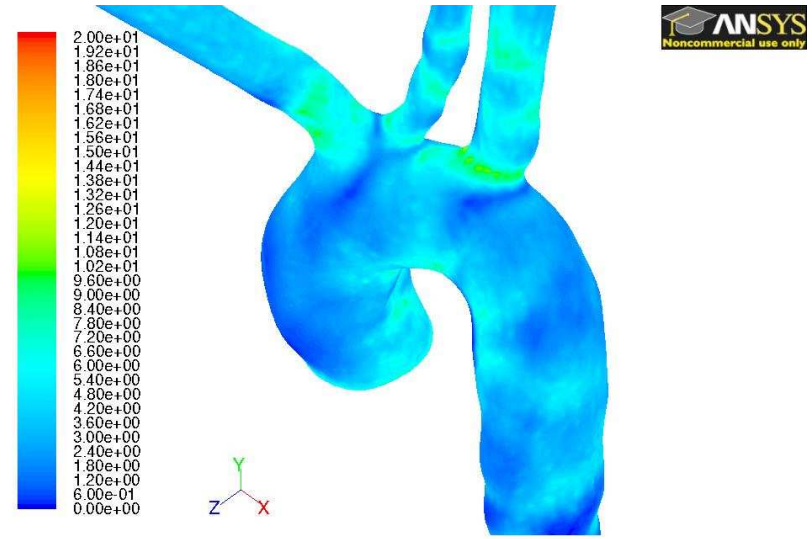

Contours of Wall Shear Stress (pascal)

May 03, 2011
ANSYS FLUENT 12.1 (3d, dp, pbns, lam)

3D PC MRI measured profile

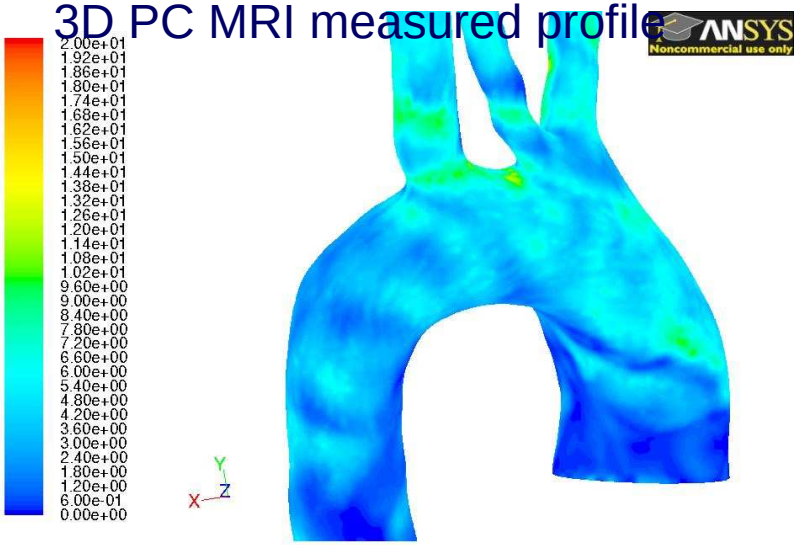

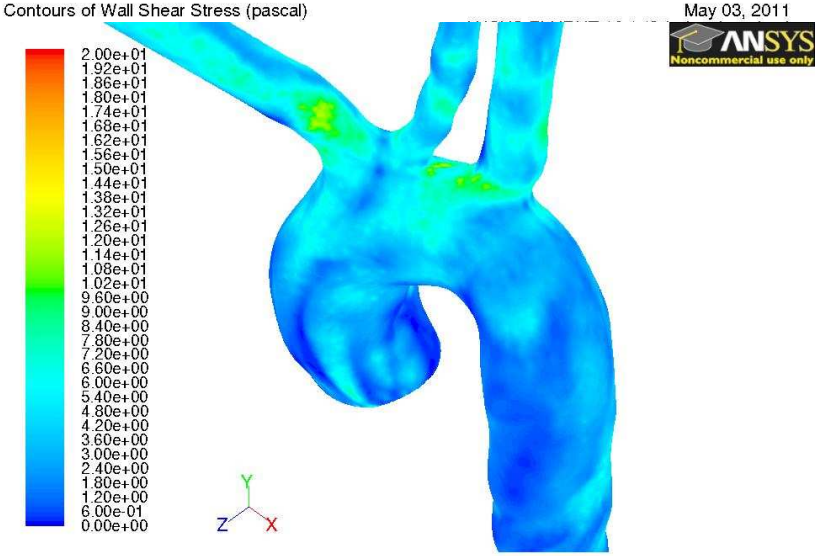

Contours of Wall Shear Stress (pascal)

May 03, 2011
ANSYS FLUENT 12.1 (3d, dp, pbns, lam)

Methods – Inlet Boundary Conditions

Inlet section AAo Velocity vectors

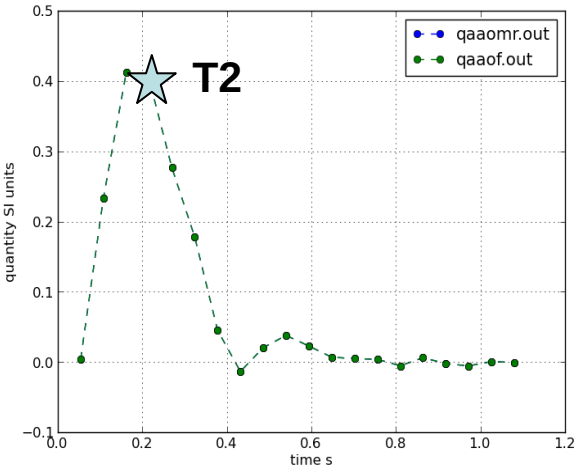

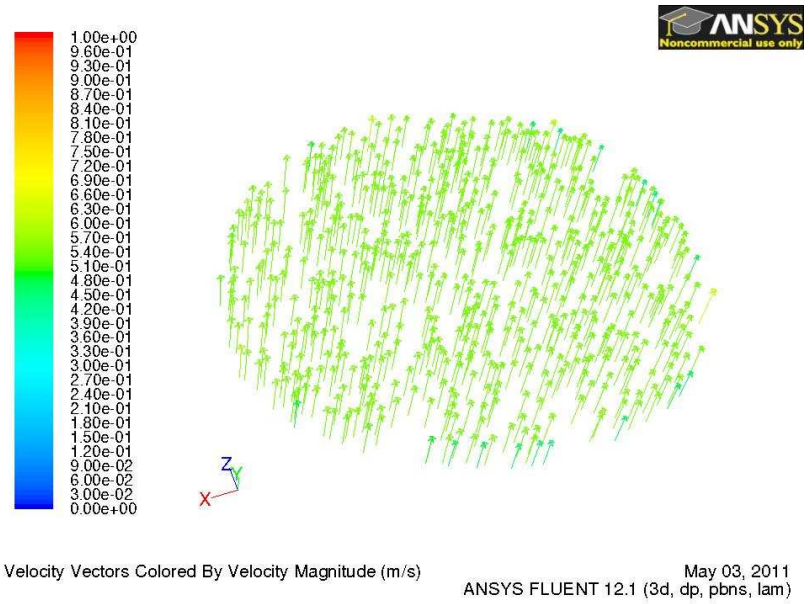

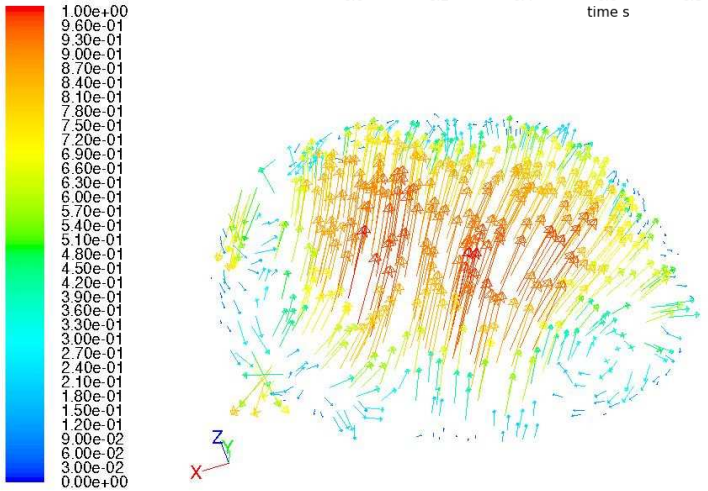

Flat V profile

3D PC MRI measured profile

Results – Streamlines at T2

Flat V profile

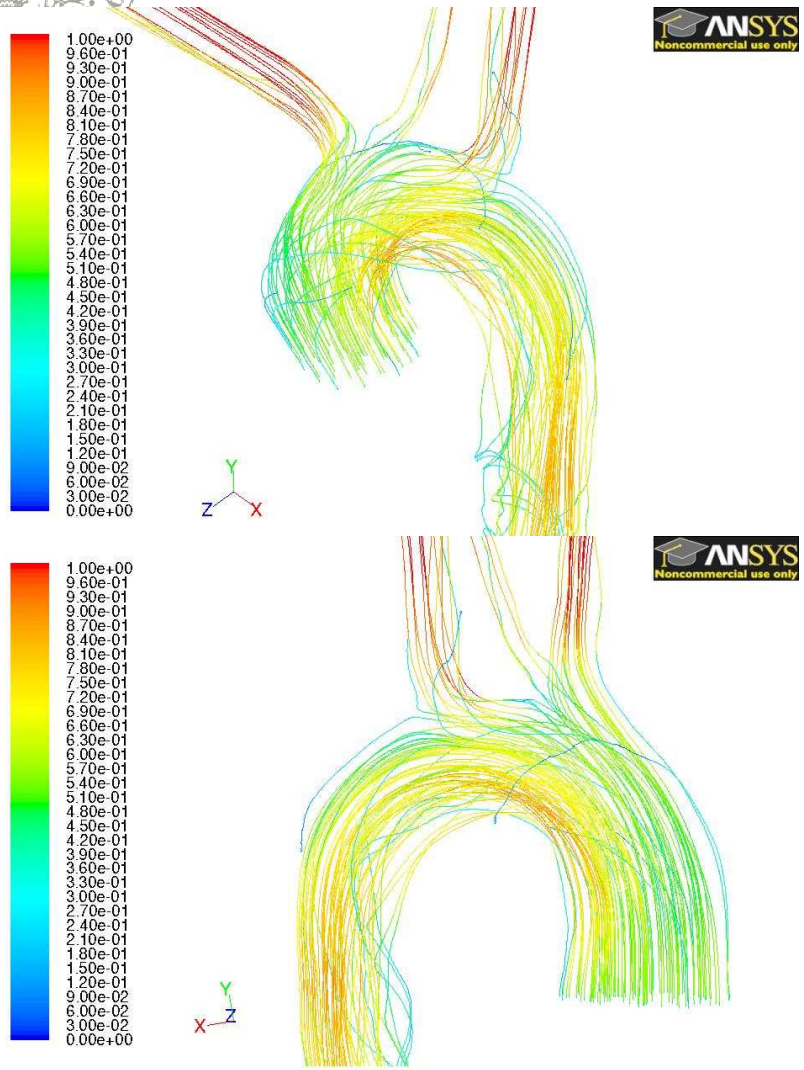

Pathlines Colored by Velocity Magnitude (m/s)

May 03, 2011
ANSYS FLUENT 12.1 (3d, dp, pbns, lam)

3D PC MRI measured profile

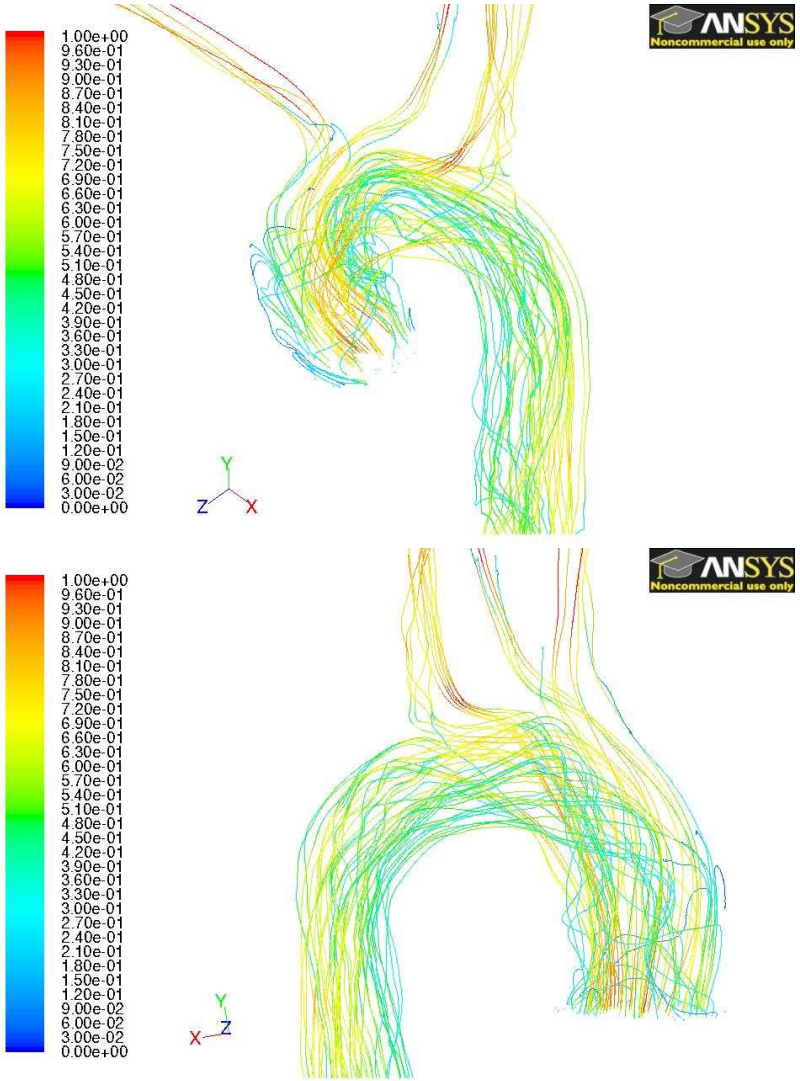

Pathlines Colored by Velocity Magnitude (m/s)

May 03, 2011
ANSYS FLUENT 12.1 (3d, dp, pbns, lam)

Results – WSS at T2

Flat V profile

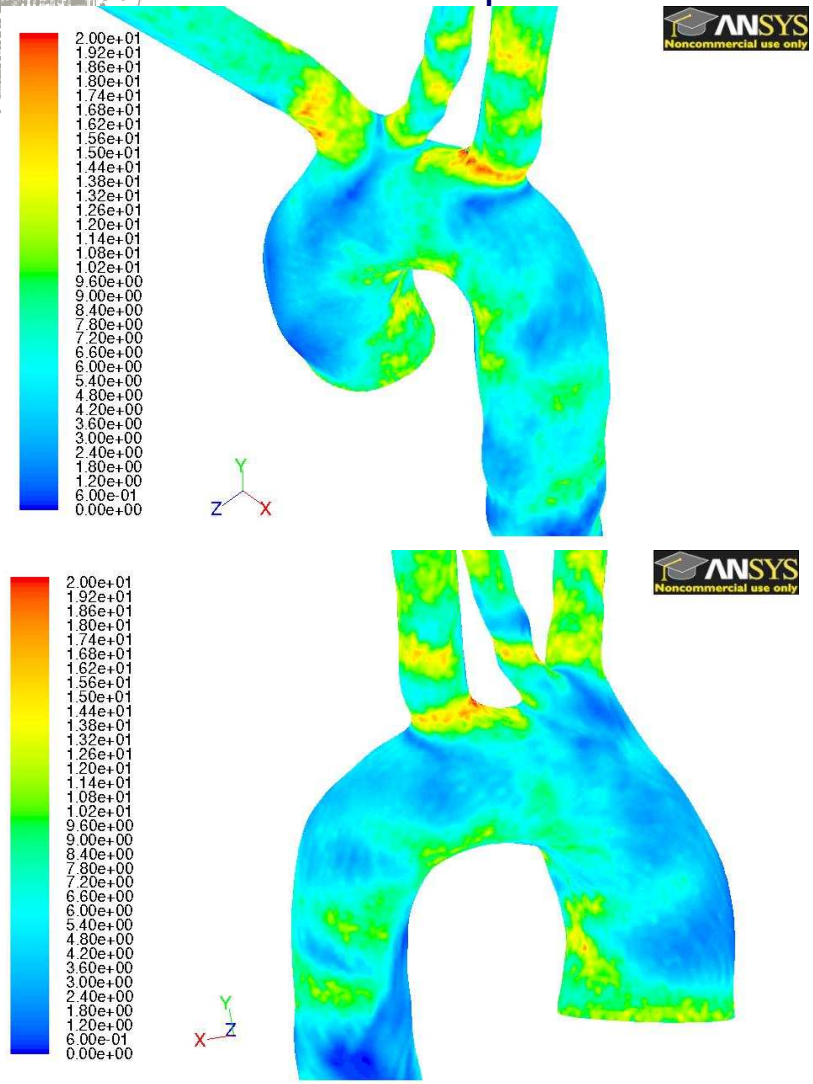

Contours of Wall Shear Stress (pascal)

May 03, 2011
ANSYS FLUENT 12.1 (3d, dp, pbns, lam)

3D PC MRI measured profile

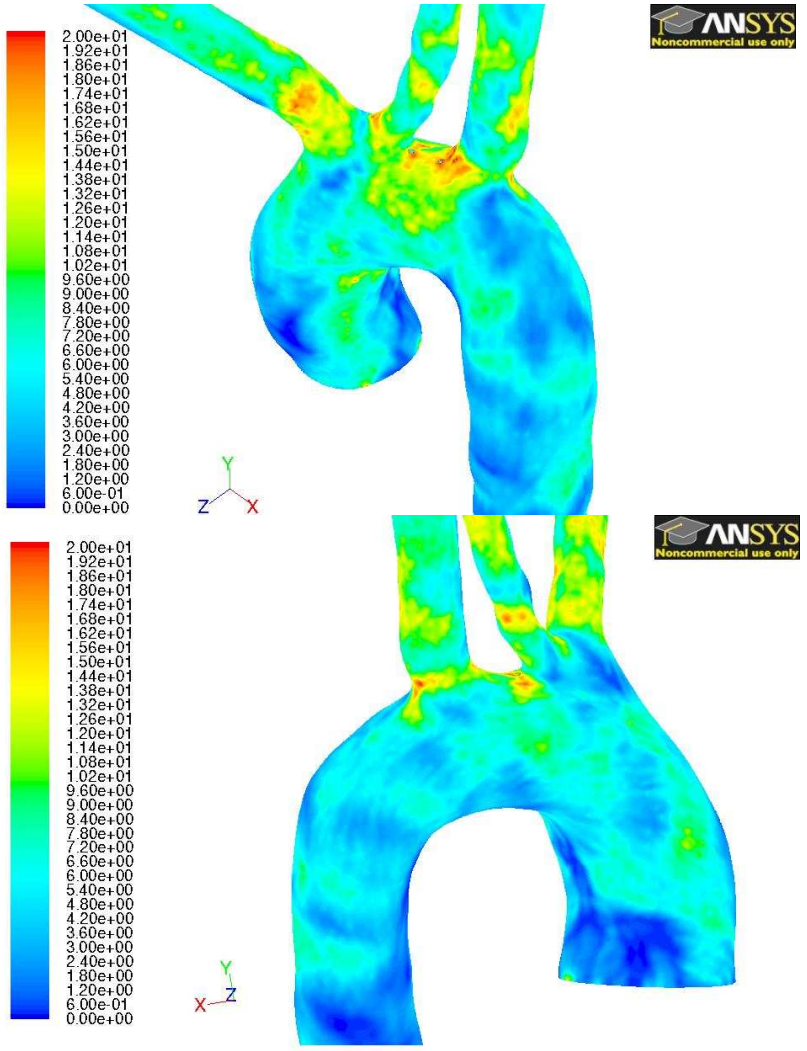

Contours of Wall Shear Stress (pascal)

May 03, 2011
ANSYS FLUENT 12.1 (3d, dp, pbns, lam)

Conclusions

From preliminary analysis

- Inlet velocity profiles seem to influence both bulk flow and WSS distribution

WORK IN PROGRESS

Thank You for Your Kind Attention

Turin Biomechanics Ramblers

Franco Maria Montevecchi

Umberto Morbiducci

Diana Massai

Diego Gallo

Francesco Mastrangelo

Francesco Pennella

umberto.morbiducci@polito.it